Journal of Archaeological Science 190 (2026) 106570

Contents lists available at ScienceDirect

Journal of Archaeological Science

journal homepage: www.elsevier.com/locate/jas

A morphological and chemo-taxonomic approach to characterize starches from plants potentially available in the Eurasian Steppe during MIS 3 (60-25 ka BP)

C. Cagnato [a,b,1], G. Sorrentino [a,1], A. Bonetto [a], F.C. Izzo [a], A. Brunelli [a], G. Birarda [c], L. Vaccari [c], S. Condemi [b], A. Carbone [d,e], A. Marcomini [a], L. Longo [a,*], E. Badetti [a,**]

[a] DAIS, Department of Environmental Sciences, Informatics and Statistics, Ca' Foscari University of Venice, Via Torino 155, Mestre, Venice, 30172, Italy
[b] UMR 7268, Anthropologie Bio-Culturelle, Droit, Ethique et Santé (ADES), 51 Bd Pierre Dramard, Marseille, 13015, France
[c] Elettra-Sincrotrone Trieste, S.S. 14 - km 163,5 in Area Science Park, Basovizza, Trieste, 34149, Italy
[d] Sorbonne Université, CNRS, IBPS, Laboratoire de Biologie Computationnelle, Quantitative et Synthétique-UMR 7238, Paris, France
[e] Institut Universitaire de France, France

ARTICLE INFO

Keywords:
Starch grains
Paleolithic
SEM
Ground stone tools
Fourier transform infrared spectroscopy
Gas chromatography-mass spectrometry
Physicochemical characterization

ABSTRACT

Plants are often underrepresented in archaeological reconstructions of past subsistence strategies, especially concerning the Paleolithic, largely because they preserve poorly in the archaeological record. However, plants are versatile resources that were used for a wide range of purposes, including as a crucial food source. Starch, a high-energy polysaccharide produced by plants, may have played an important role in the survival of *Homo sapiens* as they dispersed into the northern latitudes of Eurasia during Marine Isotopic Stage 3 (MIS 3, 60–25 ka BP). Starch granules provide direct evidence of the consumption and intentional elaboration of starchy plants. The presence of these residues alongside use-wear traces strongly suggests the deliberate exploitation of plants through mechanical processing, shedding light on early human adaptation strategies.

The conventional approach to starch grain identification relies on optical microscopy under transmitted and polarized light to detect key diagnostic features, and typically, morphological assessment is supported by comparison with modern reference collections. However, the majority of datasets prioritize economically important domesticated plants, leaving starches from wild plants available during MIS 3, particularly at boreal latitudes, largely underrepresented.

This study comprehensively analyzes starch extracted from 26 plant taxa. To this end, an array of physicochemical characterization techniques was integrated, including optical microscopy, scanning electron microscopy, laser granulometry, infrared spectroscopy, and gas chromatography-mass spectrometry. This innovative approach facilitates the identification of starch grains that are comparable to those recovered from ground stone tools at Upper Paleolithic sites across Eurasia, offering a more complete framework for archaeological interpretation.

1. Introduction

Plants have always played a relevant role for humankind, yet their significance during the Paleolithic remains difficult to assess due to their poor preservation and the small size of residues, often eluding effective analysis through traditional archaeological practices. To date, the presence of plants in such contexts have been documented through macrobotanical remains (charcoal, seeds, parenchymatous remains of tubers and rhizomes) (Mason et al., 1994; Weiss et al., 2008; Wollstonecroft et al., 2008; Pryor et al., 2013; Larbey et al., 2019; Wadley et al., 2020), microbotanical residues such as pollen, phytoliths (Madella et al., 2002; Piperno et al., 2004; Ivanova et al., 2016; Zanina et al., 2021), starches (Revedin et al., 2010; Liu et al., 2013; Power et al., 2014; Dubreuil and Nadel, 2015; Mariotti-Lippi et al. 2015, 2023; Barton et al.,

* Corresponding author.
** Corresponding author.
E-mail addresses: laura.longo@unive.it (L. Longo), elena.badetti@unive.it (E. Badetti).
[1] The authors contributed equally to this work.

https://doi.org/10.1016/j.jas.2026.106570
Received 6 October 2025; Received in revised form 1 April 2026; Accepted 8 April 2026

2018; Longo et al. 2021, 2022; Hayes et al., 2022), and, more recently, ancient plant DNA (Willerslev et al., 2014; Stahlschmidt et al., 2019; ter Schure et al., 2022). The study of these remains has provided crucial insights into how plants were exploited for subsistence strategies already in the Lower Paleolithic (Goren-Inbar et al., 2002; Ahituv et al., 2024). In the course of later periods, findings indicate a wider use of plants by modern humans, namely as sources of food (Mercader, 2009; Revedin et al., 2010; Aranguren et al., 2011; Florin et al., 2022; Hayes et al., 2022), medicines, dyes, glue, fuel, and clothing (Langejans, 2006; Hardy, 2018; Hardy et al., 2018; Sukenik et al., 2021; Longo et al., 2025), and in the creation of objects such as ropes, strings, nets, baskets, etc. (Adovasio et al., 1996; Hather and Mason, 2002; Soffer, 2004; Hardy, 2008; Hurcombe, 2014; Ingold, 2012; Hardy et al., 2020). Despite recognizing the presence of plants in contexts associated with *Homo sapiens* (*HS*), their intentional transformation for different uses is not always easily demonstrable. This is particularly true of microbotanical residues (García-Granero, 2020; Henry, 2020). Indeed, pollen is often dispersed by wind and water, even across long distances, and thus generally reflects regional vegetation, whereas phytoliths—microscopic silica structures that form within plant tissues—tend to remain in place after the plant decomposes due to their resistance to decay, and therefore are more indicative of past local vegetation and surrounding landscape (e.g., Piperno, 2006; Daniau et al., 2019; Wang et al., 2022; Olatoyan et al., 2023). On the contrary, starch grains are less prone to natural dispersal than pollen. Thus, when retrieved from the surfaces of archaeological ground stone tools (GSTs) used to mechanically process vegetal resources, it is possible to hypothesize that they are residues of this transformative activity (Mercader, 2009; Revedin et al., 2010; Barton et al., 2018; Copeland and Hardy, 2018; Kovárník and Beneš, 2018; Hayes et al., 2022). Starch has also been found in dental calculus (Hardy et al., 2009; Henry et al., 2014) and feces (Sistiaga et al., 2014). Overall, their analysis provides further evidence of their intentional human processing and consumption, and it is therefore a powerful anthropogenic proxy.

Starch is the primary polysaccharide reserve of plants, and according to the plant life cycle it can be classified as transient short-term starch, which is produced and stored in non-storage tissues such as leaves and stems and is rapidly mobilized for metabolic needs, and long-term storage starch, which accumulates in the amyloplasts of dedicated storage organs. These include above-ground storage organs (ASOs), particularly seeds and fruits, and underground storage organs (USOs) such as tubers, rhizomes, roots, and corms (Haslam, 2004). They have high energetic value, which can play a crucial role in the survival of animals capable of metabolizing them, including modern humans. Thus, starch-rich plants could have been a source of food for *HS* between 60 and 25 kya (Marine Isotopic Stage 3, MIS 3 hereafter) during its dispersal into a new environment, Eurasia, at a time of climatic harshening (Carbone et al., 2025). The chronological time frame for the present study is a constraining point as few starch-rich wild cereals were available under the severe climatic conditions that persisted until the end of the Last Glacial Maximum (Richerson et. al., 2001; Riehl et al., 2024). Therefore, it is plausible that starch was exploited by processing the storage organs from other plants, including rhizomes, tubers, shelled fruits, bark, and seeds.

Starch grains are micrometric in size (1 to 100 μm) and are characterized by concentric rings of amylose (20-30%) and amylopectin (70-80%) layered around a nucleation center called the hilum. These can be retrieved from GSTs involving wet extraction (either pipetting or sonicating the stone tool) or mechanical action using dental scalers (Mercader et al., 2018; Longo et al., 2022). Additionally, the peel-off action of silicone derivatives, often used as molds for replicating stone surface texture and studying use-wear traces, can also be utilized to recover organic residues from GST surfaces (Longo et al., 2021). Following their isolation from any associated matrix, they are commonly identified by means of optical transmitted microscopy (OM) with brightfield and polarized light (Piperno and Holst, 1998; Haslam, 2004; Piperno et al., 2004; Henry et al., 2014; Cagnato and Ponce, 2017; Copeland and Hardy, 2018; Kovárník and Beneš, 2018; Longo et al., 2021), the latter used to evidence the Maltese cross, which is a feature that appears due to their semi-crystalline structure. The morphology of starch grains can also be investigated by means of Scanning Electron Microscopy (SEM), typically providing high magnification and resolution of external features (Cortella and Pochettino, 1994; Torrence, 2006; Longo et al., 2021, 2022; Zanina et al., 2021; Birarda et al., 2023). Microscopy can also inform on mechanical processing and thermal treatment, and help identify starch granules that have been degraded by enzymatic activity, particularly due to alpha-amylase (Moss, 1976; Gott et al., 2006; Hardy et al., 2009; Ma et al., 2017). Complementarily, spectroscopic and spectrometric analysis can provide information about ancient starch composition and its structure (Birarda et al., 2023; Ordoñez-Araque et al., 2024).

These techniques can inform about other less abundant components of starch, offering additional information about their potential plant source. These components include proteins and lipids that can be found on both the surface and the interior portion of the starch grain (Pérez and Bertoft, 2010). The surface lipid components include free fatty acids, along with triglycerides, glycolipids, and phospholipids, while internal lipids are predominantly monoacyl lipids (Gallant et al., 1997; Dhital et al., 2019; Ordoñez-Araque et al., 2024). Fatty acids play a critical role in numerous biological functions that are essential for maintaining health (Ursin, 2003; Calder, 2015), including serving as an energy source (Lunn and Theobald, 2006; Ameur et al., 2012).

However, some of these spectroscopic and spectrometric techniques cannot be applied to archaeological samples since the limited amount of starch retrieved represents a constraint (Copeland and Hardy, 2018). Nevertheless, the use of brighter sources, as lasers or Synchrotron Radiation, coupled with advanced spectromicroscopies enables the analysis of even single granules (Birarda et al., 2023).

Currently, although not with the same taxonomic precision as for pollen, starch grains can be classified according to their morphology and size, which vary according to their taxa and to the different storage organs from which they originate (Esau, 1977; Pearsall, 2000). An important number of publications focus on the characterization of starches from plants of industrial interest (i.e., potato, rice, maize, manioc) (Deka et al., 2024; Shetty et al. 2024), thus limiting the proper taxonomic attribution of archaeological starch grains (but see Piperno and Holst, 1998; Messner, 2011; Mercader et al., 2018; Larbey et al., 2019; Cagnato et al., 2021; Ahituv and Henry, 2022). This scarcity of comparative datasets contributes to an incomplete picture of plant availability and use during MIS 3 at the boreal latitudes (Revedin et al., 2010; Mariotti Lippi et al., 2015; Longo et al., 2022; Birarda et al., 2023). Addressing this gap is essential, and it provided the motivation for developing a robust and systematically designed reference collection of plant starches. In this study, we present a first attempt at establishing a well-documented, multi-analytical reference framework for plants that were likely available across the Eurasian Steppe during MIS 3. This approach supports morphological comparison and also lays the groundwork for preliminary physicochemical studies.

In this context, we developed a reference collection of starch extracted from 26 plants: 23 were selected as putatively available across the Eurasian Steppe during MIS 3, and 3 non-native ones were used for comparative purposes (Hardy, 2010; Blinnikov et al., 2011; Magyari et al., 2014). The plant organs selected for the reference collection included both USO and ASO. Afterwards, a procedure to extract starches from the storage organs was developed. The isolated starch grains were morphologically analyzed using both OM and SEM. To further strengthen the analytical depth of the reference collection, we investigated starch grain size distribution using laser granulometry and characterized their chemical profiles through Fourier Transform Infrared (FTIR) Spectroscopy and Gas Chromatography-Mass Spectrometry (GC-MS). Together, these complementary methods establish an integrated comparative framework that enhances the reliability of identifying archaeological starches and represents a significant contribution toward reconstructing plant exploitation in our area of interest.

Finally, to evaluate and refine the applicability of this approach we included archaeological starch grains recovered from ground stone tools BZ833 and BZ442, unearthed from the Upper Paleolithic level of Brînzeni I Cave in Moldova (Allsworth-Jones et al., 2018). Given that it is not always feasible to perform all possible physicochemical analyses on these unique samples, we managed to combine data from OM, SEM, and FTIR. Finally, it was not possible to apply GC-MS to our archaeological samples, because although this technique requires small amounts, these are greater than those typically available to archaeologists. Moreover, given the destructive nature of this technique we used it as a complementary source of information to help interpret or confirm signals observed in FTIR spectra, particularly by identifying specific fatty acids trapped within the starch whose characteristic vibrational modes might be observed in archaeological samples.

2. Materials and methods

2.1. Plant selection based on archaeological and ethnobotanical data

In-depth analyses were performed on twenty-three plant species selected based on three criteria: the first group comprises species reported in Paleolithic archaeological contexts; a second group is composed by plants that are present up to MIS 3 in the reference region; while the last group is represented by plants that are present nowadays in regions that are known to have been crossed by *HS* 60,000 years ago, hypothesizing —if present— their past dietary exploitation. This selection was based on archaeobotanical evidence reported in the literature, including the presence of macro- and microbotanical remains (pollen, starch grains), and plant DNA (Table 1). Additionally, three species, non-native to our region of interest, were also considered for comparison, and are discussed further below. Overall, this corpus consists of 26 taxa representing 17 plant families. Both USOs and ASOs are present, with 14 USO and 13 ASO. *Isatis tinctoria* is the only species represented by two different plant parts (roots and leaves) (Table 2).

Three additional plants were considered in the reference collection, these include maize (*Zea mays*), potato (*Solanum tuberosum*), and emmer wheat (*Triticum dicoccum*). Maize was domesticated in Mexico (Piperno and Flannery, 2001), while emmer, a hulled wheat, was domesticated in the Fertile Crescent (Middle East) (Iob and Botigué, 2023). Both these plants are commonly consumed today and could thus potentially be present as contaminants in archaeological samples. The potato, originally from the Andean region (Pearsall, 2008), was chosen as a standard for several reasons, namely that it produces large, recognizable starch grains, and given that the starches are easy to extract, we were able to obtain a clean, pure starch sample.

2.2. Sampling area for the plant collection

The plants/taxa reported in Table 2 were sampled over two years in various environmental contexts. The botanical garden in Novezzina (Verona, Italy)[2] located at 1232 m asl on the Monte Baldo (Venetian Prealps), is a biodiversity hotspot, where around 50% of Alpine flora can be found. The flora of Monte Baldo, well known since the XVI century, was named *Hortus Europae* and was recognized in scholarly publications such as F. Calzolari's (2026) *Viaggio del Monte Baldo* and in the *Illustrated Flora of the Monte Baldo* (Prosser et al., 2009). Other plants were collected in the area of Marano di Valpolicella (CSI IT3210002, Verona) and in the *Busatello* freshwater swamp area,[3] which is located at the confluence of the Tione and Tartaro Rivers. Sampling was also carried out in the vicinity of Vindjia Cave (Northern Croatia) and Brînzeni I Cave (Northern Moldova), where *Heracleum sibiricum* and *Typha latifolia* were collected. Finally, the plants used as controls were purchased from local markets in Venice, Italy.

2.3. Procedure for starch extraction

2.3.1. Modern starch extraction

Five grams (or multiple aliquots) of each raw storage organ were ground by means of a blender and the chopped residue was soaked in 200 mL of ultrapure water (with a resistivity of 18.2 MΩcm, obtained with the Milli-Q® system Millipore) for 3 h. The mixture was then filtered using a Millipore filtration apparatus (Merck Millipore Glass Vacuum filtration system) by using a stainless-steel support grid with pore size of 0.1 mm. The filtered water containing the starches was then centrifuged in a Jouan CR3i centrifuge (UK) at 7000 RPM (RCF = 6147) for 10 min at 20 °C; the pellet obtained by removing the supernatant was washed with 100 mL of ultrapure water and the mixture was sonicated in an ultrasound bath for 2 min before recovering the pellet by further centrifugation. The precipitated matrix was then washed with 1 mL of ethanol (EtOH; Sigma-Aldrich), followed by the sonication and centrifugation processes as described above. The recovered pellets were dried at room temperature and stored in a dark, dry place. To prevent bacterial attack and degradation we tested different solvents as described below. In general, appropriate clean-lab procedures were applied throughout, including the use of gloves, clean tools, procedural blanks, and rigorous handling practices to minimize contamination risk.

2.3.2. Influence of organic solvents on modern starch morphologies

The influence of four different organic solvents on starch morphologies was investigated to facilitate the selection of an optimal one for the extraction procedure. 200 mg of starch grains extracted from *Castanea sativa* fruits and *Cannabis sativa* seeds were dispersed in 5 mL of the 4 following solvents: EtOH, acetone, acetonitrile, and i-propanol (Merck, Sigma-Aldrich). The 8 mixtures were briefly sonicated in an ultrasound bath (1 min) before recovering the pellets by centrifugation (for 10 min, as for the extraction procedure). The precipitated pellets were dried (at room temperature) and stored under dark conditions before the analysis.

2.3.3. Archaeological starch extraction

Archaeological starches were extracted from two GSTs collected from the site of Brînzeni I (Longo et al., 2021) at the Chemistry Department of the State University of Moldova (Chişinău). Active areas of the GSTs were immersed in MQ® water and then placed in an ultrasonic bath. The suspension was subsequently centrifuged twice at 6000 RPM and the supernatant was discarded. The remaining solution was transferred to a vial with a few drops of EtOH. For observation at the OM, a few drops of the sample were placed on a glass slide, while for SEM and FTIR the samples were suctioned in 50 μL of deionized water and dropped onto CaF_2 or ZnSe windows.

2.4. Analytical techniques used to characterize starches

2.4.1. Microscopy

An aliquot of around 1 mg of reference starch was dispersed in ultrapure water and droplets of 0.5 μL were set on a microscope slide for both OM and SEM inspection.

In preparation for OM observations, a drop of 1:1 water:glycerine solution was added to the sample on the slide, before placing a cover slip on top. The slides were then viewed between 100× and 600×

[2] This area is acknowledged as a CSI Site of Community Site of Importance, IT 3210039, IT 3210004, and Rural Development Program (RDP) for the Veneto Region, 2014-2020.

[3] This area is acknowledged as a Site of Community Importance (CIIS IT3210013) and as a Special Protection Area (SPA IT3210013).

Table 1
Summary of plant taxa selected for this study, their documented regional and chronological archaeobotanical evidence, and corresponding bibliographic references.

Taxa	Region	Period	Archaeological contexts	Type of evidence	References
Arundo donax	Tajikistan	4th- end of 3rd millennia BC	Sarazm	Carbonized wood	Spengler and Willcox (2013)
Avena sativa	Israel	780 ky	Gesher Benot Ya'aqov	Grinding stones (starch grain)	Ahituv et al. (2024)
	Italy (*Avena* sp.)	33 ky	Paglicci Cave	Grinding stones (starch grain)	Mariotti Lippi et al. (2015)
	Altai in Central Eurasia (*Avena* sp.)	6th – 4th c. BC	Various sites	Dental calculus (starch grains)	Zanina et al. (2021)
Cannabis sativa	Turkey (*Cannabis* sp.)	110 kya	_	Pollen	McPartland et al., (2019); Rull (2022)
Carex humilis	Germany (*Carex* various species)	300 ka	Schoningen 13 II	Seeds and pollen	(Bigga et al., 2015); Urban and Bigga (2015)
	Eastern Russia (*Carex dioica*)	22,500 cal yr BP	Northern Yakutia	Woolly mammoth gut content (seeds)	van Geel et al. (2008)
	Poland (*Carex* sp.)	11380- 8270 BP	Całowanie	Sediment (Carbonized achenes)	Kubiak-Martens (1996)
Castanea sativa	Georgia	84-56 kya BP	Solkota Cave	Stalagmite (aDNA)	Stahlschmidt et al. (2019)
	Spain	3140 cal BP	El Tiemblo	Sediment cores (Pollen)	Lòpez-Sàez et al. (2017)
Cyclamen sp.	West Carpathians and in the Southern Limestone Alps (*C. purpurascens*)	115-11 kya	Multiple refugia	DNA	Slovak et al. (2012)
Cyperus rotundus	Germany (*Cyperus pannonicus*)	ca. 300 ka	Schoningen 13 II	_	(Bigga et al., 2015)
Convallaria majalis	Hungarian Plain	Subboreal period (5000-2500 yr BP)	Lake Balaton	Pollen	Nagy-Bodor et al. (2000)
Echinochloa crus-galli	China (*Echinocloa* spp.)	13,800 and 11,600 cal. BP	Shizitan Locality 9	Carbonized seeds	Bestel et al. (2014)
	Eastern Ukraine	5th and 1st centuries B.C.	Zanovskoe	Pits (Carbonized grains)	Motuzaite-Matuzeviciute et al. (2012)
Erythronium dens-canis	Altai in Central Eurasia (*Erythronium sibiricum*)	Early Iron Age (5th century BC – 5th century AD)	Various sites	Dental calculus (Starch grains)	Zanina et al. (2021)
	Believed to have originated in Pleistocene Europe	Currently found in evergreen taiga and montane forests, as well as coniferous forests	_	_	Hardy (2010)
Heracleum sibiricum	Czech Republic (*Heracleum* sp.)	10,500 and 7500 B.P.	Various sites	Pollen	Kuneš et al. (2008)
	Altai in Central Eurasia (*Heracleum dissectum*)	2nd c. BC – 5th c. AD	Stepuska	Dental calculus (starch grains)	Zanina et al. (2021)
Iris sibirica	Bulgaria (*Iris pumila*/*Iris gramminea)*	39 kya	Magura Cave	Hyena coprolites (Pollen)	Ivanova et al. (2016)
Isatis tinctoria	Armenia	39-24 ky	Aghitu-3 Cave	Sediment cores (DNA)	ter Schure et al. (2022)
	Georgia	32-34 ya	Dzuduana Cave	Grinding stones (starch grain)	Longo et al. (2025)
Linum usitatissimum	Georgia	84-56 kya BP	Solkota Cave	Stalagmite (aDNA)	Stahlschmidt et al. (2019)
Oxalis acetosella	Hungary	Current	_	Modern vegetation	Dénes et al. (2012)
	NW Russia	Current	_	Modern vegetation	Kolosova et al. (2020)
	Georgia	Current	_	Modern vegetation	Nakhutsrishvili et al. (2022)
Pastinaca sativa	Believed to have originated in Pleistocene Europe	Current	Currently found in evergreen taiga and montane forests, as well as coniferous forests	Modern vegetation	Hardy (2010)
Paeonia officinalis	Altai in Central Eurasia (*Paeonia anomala*)	Early Iron Age (5th century BC – 5th century AD)	Various sites	Dental calculus (starch grains)	Zanina et al. (2021)
Pisum sativum[a]	Armenia	39-24 ky	Aghitu-3 Cave	Sediment cores (DNA)	ter Schure et al. (2022)
	Southern Levant (*Pisum* sp.)	ca. 10300-9000 BC	Hayonim Cave	Seeds (attributed to)	Hopf and Bar-Yosef (1987)
	Altai in Central Eurasia	5th c. BC – 5th c. AD	Various sites	Dental calculus (starch grains)	Zanina et al. (2021)
Quercus ilex	Israel	780 kya	Gesher Benot Ya'aqov	Grinding stones (starch grains)	Ahituv et al. (2024)
	Armenia (*Quercus* sp.)	39-24 kya	Aghitu-3 Cave	Sediment cores (DNA)	ter Schure et al. (2022)
	Italy (Deciduous *Quercus*)	Aurignacian and Gravettian levels	Paglicci Cave	Charcoal	Mariotti Lippi et al. (2015)
Rumex acetosa	Germany (*Rumex maritimus*)	Ca. 300 ka	Schoningen 13 II	macro-remains	(Bigga et al., 2015)
	Eastern Russia (*Rumex* cf. *sibirica*)	39140 ± 390 years ago	Cherskii	Woolly rhinoceros gut contents (pollen)	Boeskorov et al. (2011)
	Armenia (*Rumex sculatus*)	39-24 kya	Aghitu-3 Cave	Sediment cores (DNA)	ter Schure et al. (2022)
	Balkans (*Rumex acetosa*)	39.300 ± 50 ka	Magura cave	Coprolites (pollen)	Ivanova et al. (2016)
	Eastern Russia (*Rumex acetosella*)	22,500 cal yr BP	Northern Yakutia	Woolly mammoth gut contents (seeds, pollen)	van Geel et al. (2008)

(continued on next page)

Table 1 (*continued*)

Taxa	Region	Period	Archaeological contexts	Type of evidence	References
Sagittaria sagittifolia	Israel (*Sagittaria* sp.)	700 and 800 kya	Gesher Benot Ya'aqov	Pollen	van Zeist and Bottema (2009)
	Germany	ca. 300 ka	Schoningen 13 II	Pollen	(Bigga et al., 2015)
	Poland	9390 ± 70 B.P.	Całowanie	Sediments (tubers)	Kubiak-Martens (1996)
Sorghum halepense	Believed to be native to Western Asia	Current	_	_	Paterson et al. (2020)
Typha latifolia	Germany (*Typha* sp.)	ca. 300 ka	Schoningen 13 II	Seed and rhizomes	(Bigga et al., 2015)
	Armenia (*Typha* sp.)	39-24 kya	Aghitu-3 Cave	Sediment cores (DNA)	ter Schure et al. (2022)
	Italy (*Typha* sp.)	Gravettian	Bilancino II	Pollen	Revedin et al. (2010)

[a] DNA from Aghitu-3 Cave has been attributed to pea (*Pisum sativum;* ter Schure et al., 2022). However, these data seemingly contradict the well-established early Holocene timing of pea domestication, which occurred around 10,000 BC in the Near East and in Central Asia. Earlier Pleistocene occurrences of *Pisum* in the eastern Mediterranean-Near Eastern region likely relate to wild taxa (e.g. *P. sativum* ssp. *elatius*, *P. fulvum*) and not to the cultivated form of *P. sativum sensu stricto* (Trněný et al., 2018).

Table 2
Plants selected for this study, potentially available during MIS 3 (Entries 1-24) and reference materials or potential contaminants (Entries 25-27).

	Name	Common name	Family	Plant part	Storage organ
1	*Arundo donax* L.	Giant cane	Poaceae	Stalk	ASO
2	*Avena sativa* L.	Oat	Poaceae	Seed	ASO
3	*Cannabis sativa* L.	Hemp	Cannabaceae	Seed	ASO
4	*Carex humilis* Leyss.	Lesser pond-sedge	Cyperaceae	Seed	ASO
5	*Castanea sativa* Mill.	Chestnut	Fagaceae	Fruit	ASO
6	*Cyclamen* sp.	Cyclamen	Primulaceae	Root	USO
7	*Cyperus rotundus* L.	Purple nut sedge	Cyperaceae	Rhizome	USO
8	*Convallaria majalis* L.	Lily of the Valley	Asparagaceae	Root	USO
9	*Echinochloa crus-galli* (L.) P. Beauv.	Cockspur	Poaceae	Seed	ASO
10	*Erythronium dens-canis* L.	Dog's-tooth-violet	Liliaceae	Bulb	USO
11	*Heracleum sibiricum* L.	Cow parsnip	Apiaceae	Root	USO
12	*Iris sibirica* L.	Iris	Iridaceae	Root	USO
13	*Isatis tinctoria* L.	Woad	Brassicaceae	Leaf	ASO
14	*Isatis tinctoria* L.	Woad	Brassicaceae	Root	USO
15	*Linum usitatissimum* L.	Flax	Linaceae	Seed	USO
16	*Oxalis acetosella* L.	Wood sorrel	Oxalidaceae	Rhizome	USO
17	*Pastinaca sativa* L.	Parsnip	Apiaceae	Root	USO
18	*Paeonia officinalis* L.	Common peony	Paeoniaceae	Shoot	ASO
19	*Pisum sativum* L.	Pea	Fabaceae	Seeds	ASO
20	*Quercus ilex* L.	Evergreen oak	Fagaceae	Seed	ASO
21	*Rumex acetosa* L.	Curly dock	Polygonaceae	Roots	USO
22	*Sagittaria sagittifolia* L.	Arrowhead	Poaceae	Rhizome	USO
23	*Sorghum halepense* (L.) Pers.	Johnson grass	Poaceae	Seed	ASO
24	*Typha latifolia* L.	Cattail	Typhaceae	Rhizome	USO
25	*Solanum tuberosum* L.	Potato	Solanaceae	Tuber	USO
26	*Triticum dicoccum* Schrank ex Schübl.	Emmer wheat	Poaceae	Seed	ASO
27	*Zea mays* L.	Maize/corn	Poaceae	Seed	ASO

magnification by means of a polarizing microscope (Nikon Eclipse 600 EPOL). Individual starch grains were photographed using a Zeiss Axiocam 305 color camera and measured with a dedicated software.

For SEM visualization, the samples were observed without coating. Glass slides were mounted directly on the SEM holder and then observed with minimal dose and charge parameters with a high-resolution Field-Emission SEM operating at 3 kV (GeminiSEM500, Zeiss) with a 15 mm objective aperture diameter. Secondary electrons were collected with the high sensitivity Everhart-Thornley detector. Scan speed and integration mode were adjusted during observation to optimize signal detection.

2.4.2. *Laser granulometry*

Particle size analysis by laser diffraction granulometry was conducted using a Mastersizer 3000 (Malvern Panalytical) with a wet dispersion unit (Hydro EV). Starches were added to 500 mL of pure water until at least 5% obscuration was achieved. The dispersions were stirred at 2500 rpm and the ultrasonic bath was set to 90% power to ensure the deagglomeration of the starch and stability of the suspension during analysis. To enhance statistical robustness, each sample was measured for 10 s across 10 replicates. The data were processed using the instrument's software, considering the particles as "non-spherical", and selecting cellulose as the material (Adsorption Index 1.468, Refractive Index 0.01, Density 1 g/cm^3), and water as the dispersant. The results are reported as volume-based distributions in the range between 0.1 and 1000 μm.

2.4.3. *Spectroscopy*

Fourier Transform Infrared spectroscopy (FTIR) analyses were performed directly on the starches extracted from the modern plants without further preparation (Figs. S1–S27). For these samples, Thermo Nicolet Nexus 670 FTIR spectrophotometer equipped with a Smart Orbit Single Reflection Diamond ATR (Attenuated Total Reflection) accessory was used. The samples were analyzed in the 4000-400 cm^{-1} region, averaging 64 scans with 4 cm^{-1} spectral resolution.

As far as the archaeological samples are concerned, they were measured at the Chemical and Life Sciences branch of the infrared beamline at Elettra Sincrotrone Trieste, (SISSI-Bio) (Birarda et al., 2022). The samples were dropped onto 1 mm thick ZnSe IR-grade windows and analyzed using a Hyperion 3000 Vis/IR microscope coupled with a VERTEX 70v interferometer (BRUKER Optics, Billerica MA, US). Chemical images were collected using the focal plane array detector (FPA) and co-adding 256 scans for each measurement, at a spectral resolution of 4 cm^{-1}. Single spectra were extracted with OPUS 8.5 software as previously outlined in Birarda et al. (2023). FTIR data were elaborated with Omnic 9.0, OPUS 8.5, Origin 8.0, and Origin Pro 2024 software.

2.4.4. *Gas chromatography- mass spectrometry (GC-MS)*

GC-MS analyses were performed to detect and quantify fatty acids from lipids in the extracted starches. A well-established GC-MS methodology for lipidic fractions determination was adopted (Izzo et al. 2014, 2022; Scarponi et al., 2021; Fuster-López et al., 2019; Caravá et al., 2020; Gnemmi et al., 2024): small amounts of starch samples (from 0.20 to 0.40 mg) were treated with 50 μL of 2.5% in methanol, by an overnight reaction carried out at room temperature. This allows fatty acids to be transformed into their corresponding methyl esters. 1 μL of each derivatized solution was automatically injected by an autosampler AS1310 (Thermo Scientific) in a Trace GC 1300 system (Thermo Scientific) equipped with an ISQ 7000 MS detector with a quadrupole analyzer (Thermo Scientific). The chromatographic separation was obtained on a chemically-bonded fused silica capillary DB–5MS Column (30 m length, 0.25 mm, 0.25 μm—5% phenyl methyl polysiloxane), using helium as the carrier gas (flow rate 1 ml min^{-1}). The GC inlet, the MS interface, and the transfer line were maintained at 280 °C, while the MS source temperature was set at 300 °C. The temperature ramp was set from 50 (3 min) to 320 °C (5 min), 10 °C min^{-1}. The MS ran in Full Scan mode (m/z 40–650) at 1.9 scans/s. Electron ionization energy was 70 eV.

The compounds were identified by comparing them with the NIST and MS Search 1.7 libraries of MS spectra, as well as a lipid library created by the authors.

Quantitation of fatty acids in starches was achieved using nonadecanoic acid as the Internal Standard and a standard solution containing the most abundant saturated (myristic, palmitic, stearic) and unsaturated (oleic, linoleic, linolenic, palmitoleic) fatty acids. Quantitative data obtained were expressed in μg/mg.

Data from GC-MS were statistically analyzed through hierarchical clustering analysis, using the maximum distance between any two points in separate clusters to determine the distance between those clusters (called "complete" linkage). This method focuses on the furthest points, leading to more compact and well-separated clusters with respect to single or average linkage methods. Statistical analysis was performed using R Statistical Software (v4.1.2; R Core Team, 2021), using R package "hclust" (Becker et al., 1988).

3. Results and discussion

A combination of analytical techniques was used to characterize the starches extracted from the selected plants, with the aim of providing new, unexplored features that could improve the identification of plant residues obtained from archaeological materials, such as GSTs, dental calculus, and coprolites. Optical microscopy, commonly utilized by archaeologists to identify starches and other residues in a non-destructive manner, was integrated with SEM inspection, which also allowed observations of smaller remains in a more detailed way. We coupled these imaging analyses with a physicochemical characterization by means of granulometric, FTIR, and GC-MS techniques.

3.1. Extraction procedure

The starch granule extraction procedure from modern plants developed in this study (section 2.3) aimed at preserving the morphology, size, and shape of the granules. To prevent chemical degradation, a set of solvents was tested during the extraction procedure. The best option was selected after mixing the starches obtained from *Castanea sativa* and *Cannabis sativa* with four different solvents, and analyzed by OM and SEM. Due to the small size of the *Cannabis sativa* starch grains, we were unable to document any morphological modifications by OM. *Castanea sativa* starch grains observed with the OM, did not show a significant variation in shape after solvent treatment (Figs. S28–S31). However, SEM images allowed us to identify some alterations in both cases, as shown in Fig. 1. *Castanea sativa* showed starch granule degradation with all the other solvents tested except EtOH. In particular, acetone and i-propanol lead to an opening of the starch granules, exhibiting amylose and amylopectin rings. As for acetonitrile, it appears to dissolve the starch granules. Even in the case of *Cannabis sativa* starches, except for EtOH, granule alteration was observed with all the solvents used. Accordingly, EtOH was selected as the most suitable solvent to be used following the extraction procedure of the plants reported in Table 2, which prevents bacteriological attacks without altering the shape or size of the starch granules.

3.2. Morphological characterization and size distribution

The starch granules extracted from the plants listed in Table 2 were examined by OM, where the typical Maltese cross was observed, and by SEM (Figs. 2–5). Both sets of images revealed a variety of shapes, including spherical, polyhedral, and elliptic starch grains. In some cases, other vegetal residues (i.e., raphides, amyloplasts) besides starch grains were observed; this will be further discussed in section 3.3. In the case of *Isatis tinctoria,* we only included images of the starch grains found in the root, as those in the leaves were too small to be characterized using the OM.

Avena sativa and *Arundo donax* notably produce compound starch grains, which are aggregates of individual starch grains. These aggregates are also present in other members of the Poaceae family, including rice, sorghum, and millet. We then observe starch grains that are rounder to hemispherical in shape, such as for *Carex humilis*, *Typha latifolia*, *Cannabis sativa*, and *Paeonia officinalis*. *Linum usitatissimum*, *Convallaria majalis, Echinocloa crus-galli* and *Zea mays* range from roundish to more facetted. *Sagittaria sagittifolia, Quercus ilex, Castanea sativa*, *Cyclamen*, and *Solanum tuberosum* produce starch grains that are

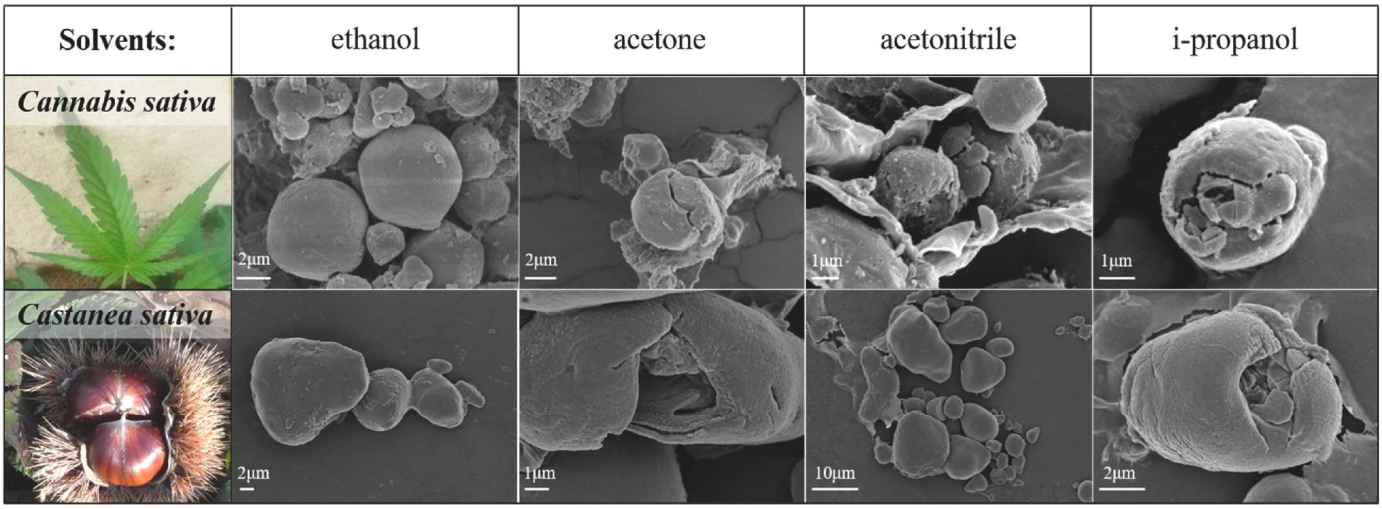

Fig. 1. SEM images of *Cannabis sativa* and *Castanea sativa* starch grains washed with different solvents.

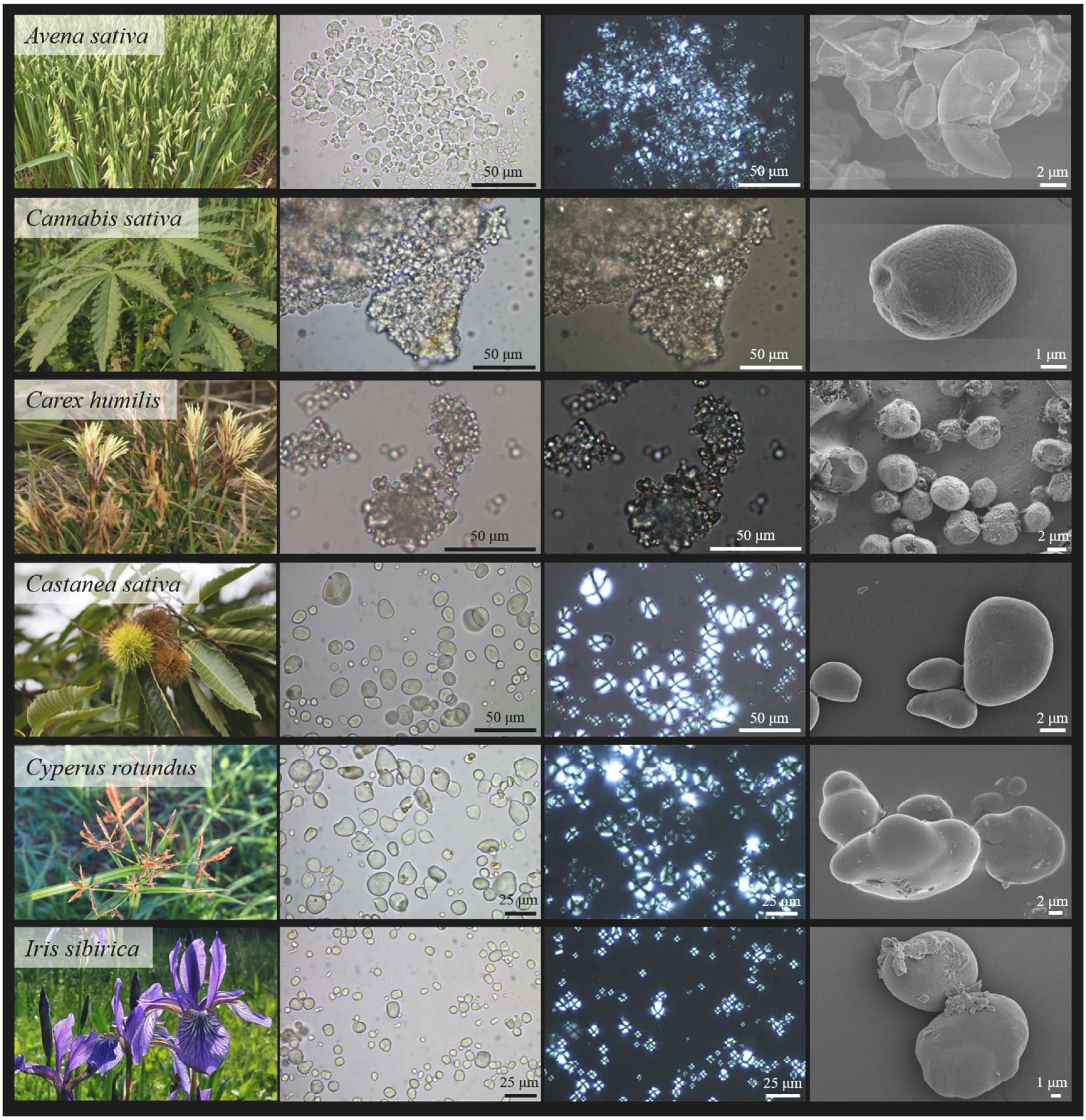

Fig. 2. Images of modern plants (first column; images downloaded and modified from https://www.gbif.org/) selected according to their presence in the archaeological record during our period of interest, and corresponding starches imaged by OM (second and third column) and SEM (fourth column).

more oval and elongate. *Erythronium dens-canis* also fits this category, although numerous grains tend to taper towards one end and are more flattened when viewed sideways. Very irregular starch grains can be found in several of our taxa, including *Iris sibirica*, *Cyperus rotundus*, *Pisum sativum, Heracleum sibiricum*, *Oxalis acetosella*, *Rumex acetosa*, and *Pastinaca sativa*. Of the taxa from this list, only *Typha latifolia* and *Convallaria* contained raphides (calcium oxalate crystals).

Starch grains produced by *Triticum dicoccum* are highly bimodal. They produce large oval grains that when viewed sideways are lenticular in shape, while the smaller grains (<10 µm) are more spherical in shape. This type of bimodal distribution is commonly seen in the Triticeae tribe (Poaceae family), notably in many domesticated species such as wheat and barley (Yang and Perry, 2013).

The size of starches analyzed by OM and SEM are depicted as boxplots in Fig. 6, ranging from 0.6 to 62 µm in length. The smaller grains belong to *Cannabis sativa*, while the potato produces the largest starch grains. It is not surprising that the size ranges obtained by OM and SEM slightly differ, given the higher magnification of SEM, capable of imaging smaller starch grains barely or not visible with OM.

Laser diffraction particle size analysis achieved further information on the size ranges, allowing the measurement of the hydrodynamic size of a large quantity of starch grains dispersed in ultrapure water. The

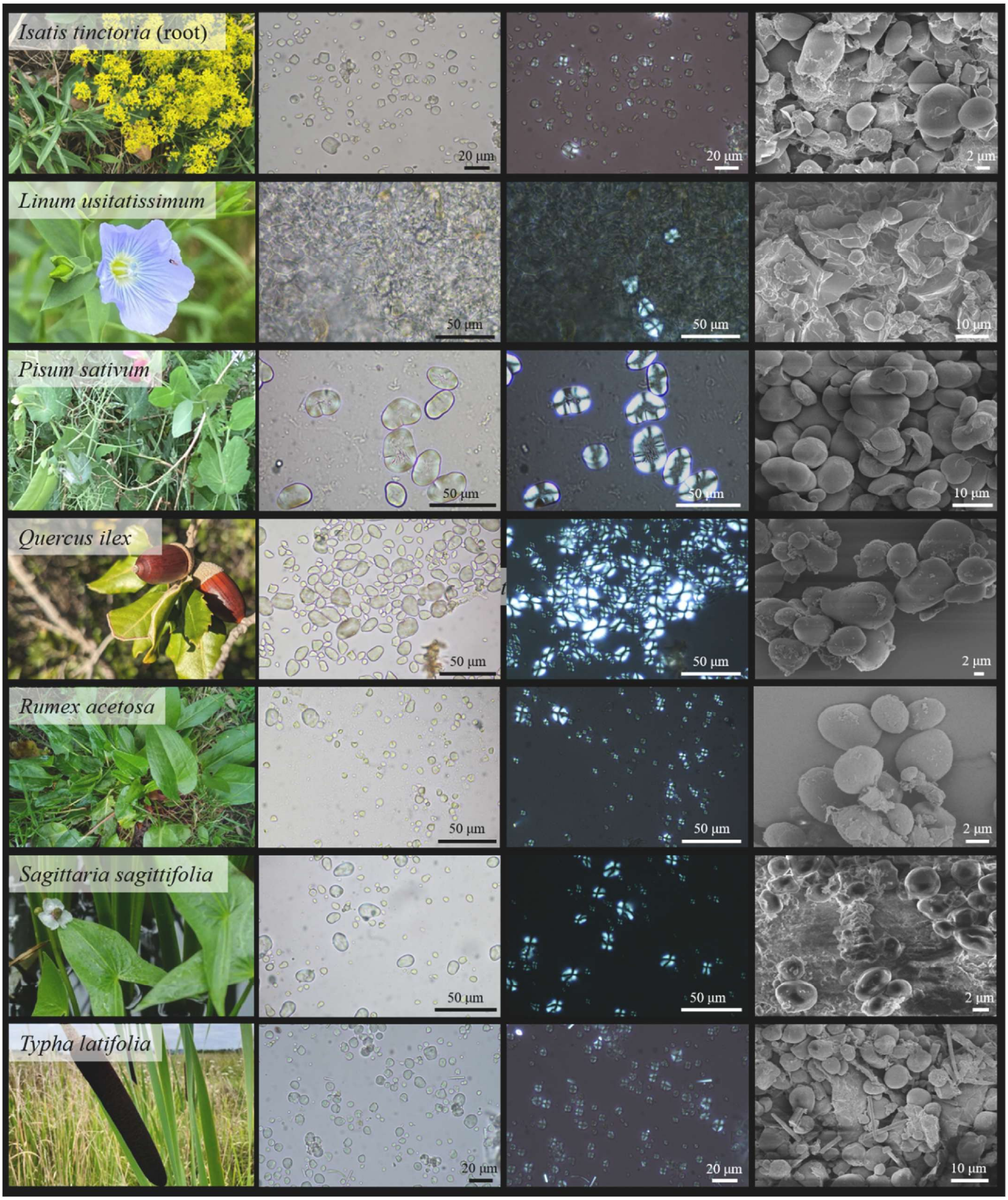

Fig. 2. (*continued*).

overall data are reported in Table S1 and once more, the measurements obtained are slightly different from the size calculated by the other techniques. This is due to the technique's physical basis: laser diffraction determines the size distribution of starch dispersed in water by measuring the scattered light as a function of the scattering angle, unlike OM or SEM techniques that image individual constituent particles (Bresch et al., 2022).

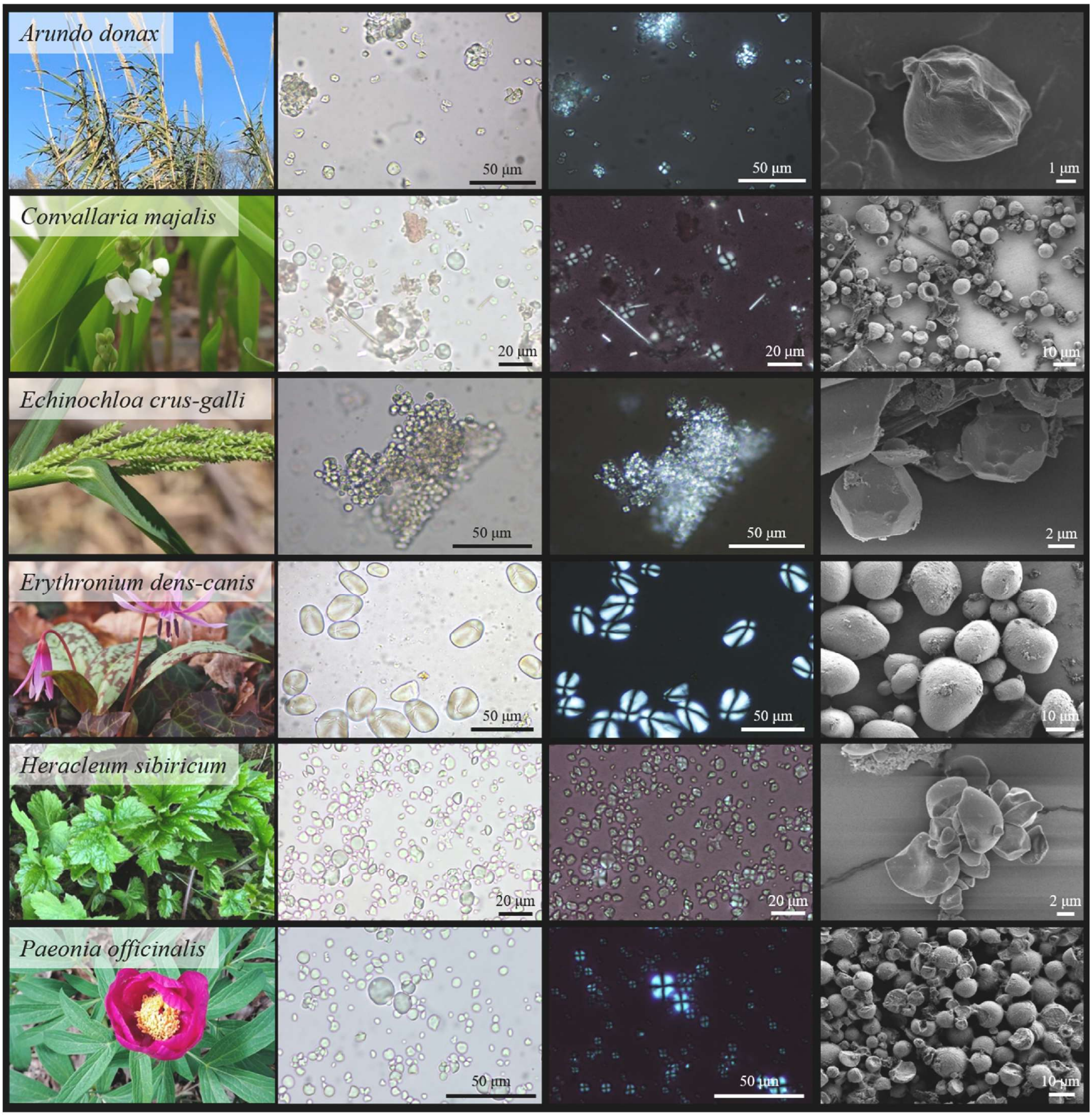

Fig. 3. Images of modern plants (first column; images downloaded and modified from https://www.gbif.org/) selected according to their presence in the archaeological record but that postdate our time period, and corresponding starches imaged by OM (second and third column) and SEM (fourth column).

3.3. FTIR characterization of extracted starches

As clearly revealed by SEM, besides the presence of starches, other organic plant residues such as raphides (calcium oxalate crystals) and phytoliths (siliceous concretions in plants) can be observed in the extracted materials. These same residues are also frequently observed in archaeological samples (Crowther, 2009; Shillito, 2018) and together with other less structured remains that cannot be easily identified using OM and SEM, or that need other analytical techniques to be detected, could provide important information about past plant use.

In this context, to strengthen our understanding of other organic residues that can remain behind with starches after the extraction procedure herein followed, FTIR analysis was performed on all the extracted starches reported in Table 2 and their corresponding spectra are reported in the SI.

Solanum tuberosum was selected as a reference material, given the purity of the starch extracted. Indeed, the corresponding FTIR spectrum (Fig. 7) showed the characteristic absorptions associated with amylose and amylopectin in the wavelength region between 3600 and 600 cm^{-1}. The typical absorption bands observed, assigned according to Monnier et al. (2017), are the following: 3249 cm^{-1} (O-H stretching), 2928 cm^{-1} (CH_2 stretching), 1640 cm^{-1} (O-H bending mode of adsorbed water),

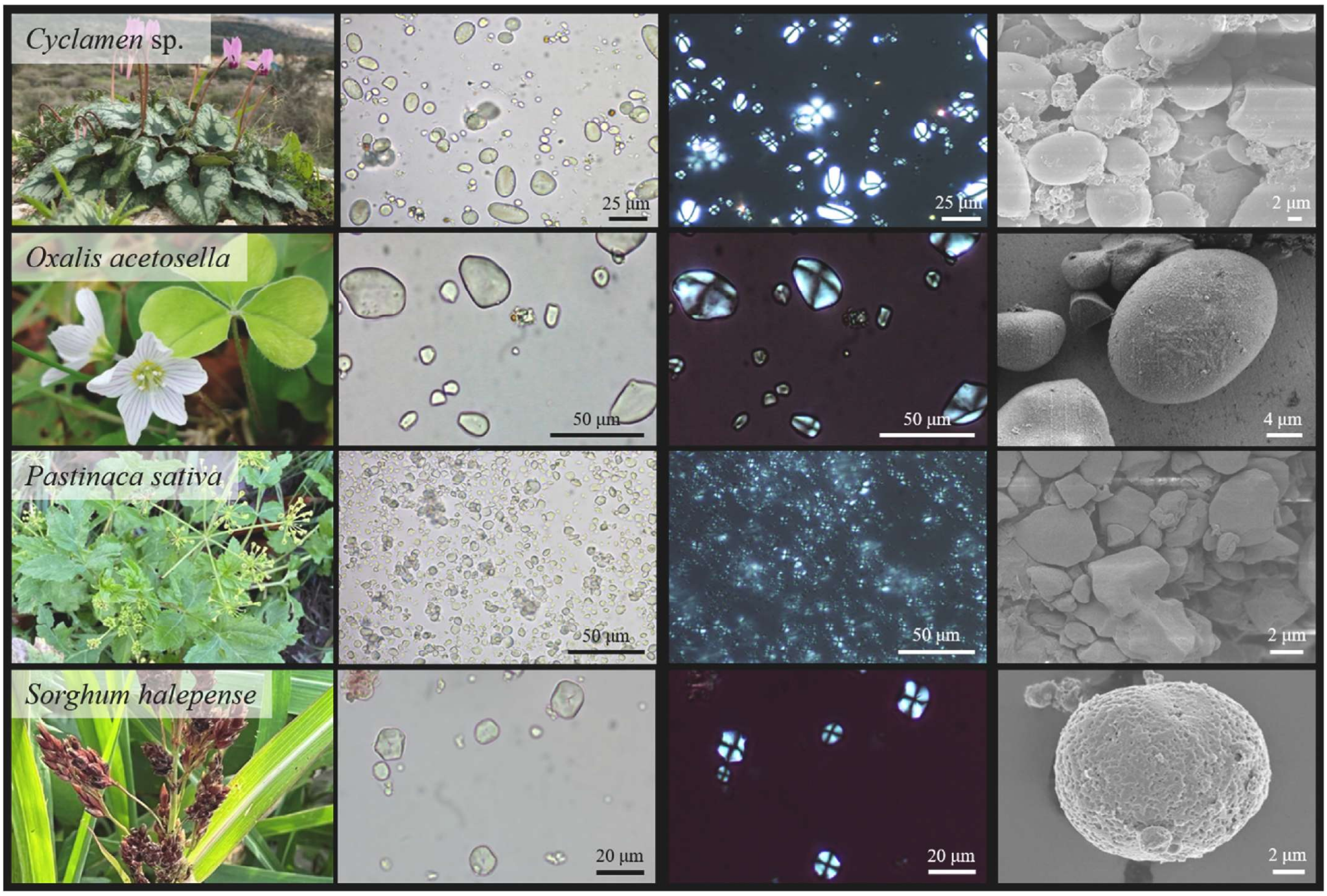

Fig. 4. Images of modern plants (first column; images downloaded and modified from https://www.gbif.org/) based on their current consumption in our region of interest, and corresponding starches imaged by OM (second and third column) and SEM (fourth column).

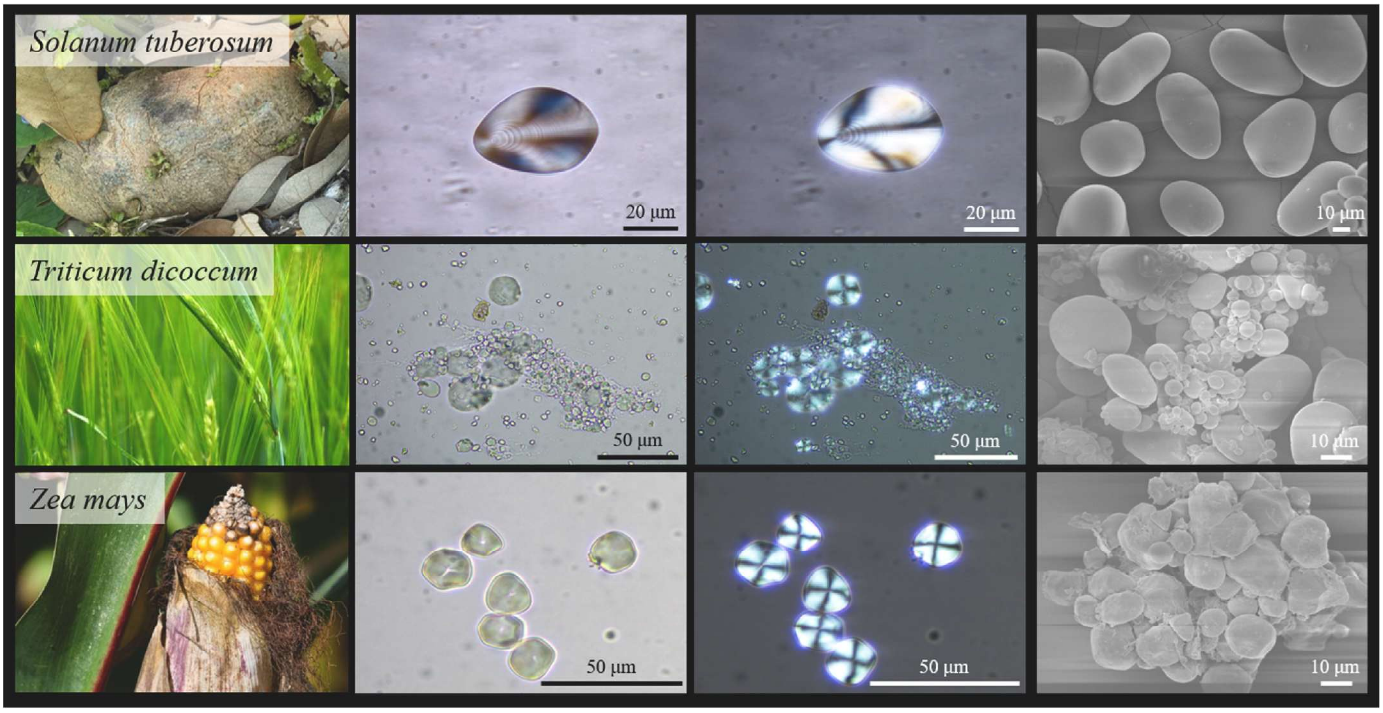

Fig. 5. Images of modern plants (first column; images downloaded and modified from https://www.gbif.org/) selected as standard (*Solanum tuberosum*) and potential contaminants (*Triticum dicoccum* and *Zea mays*), and corresponding starches imaged by OM (second and third column) and SEM (fourth column).

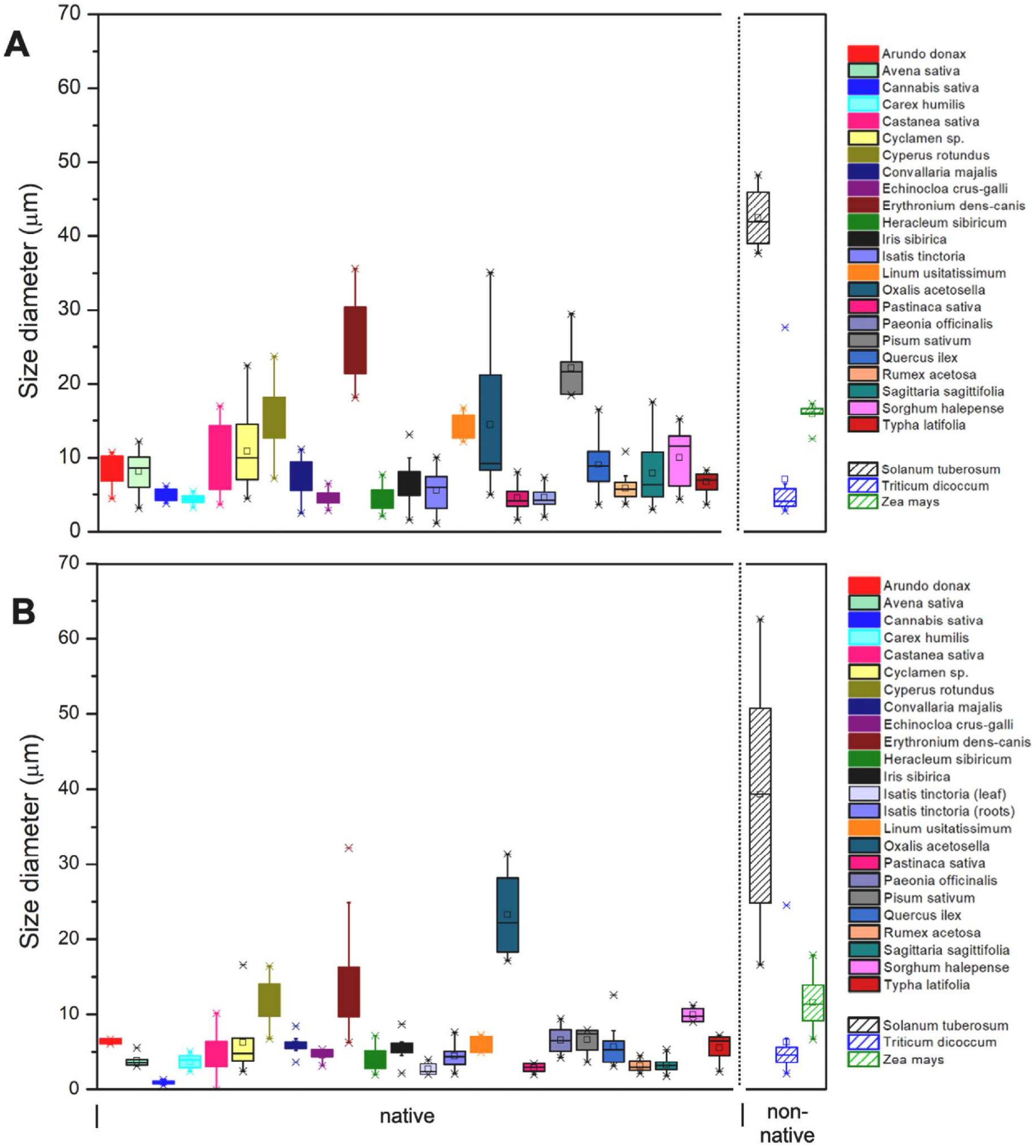

Fig. 6. Starch granule size ranges as derived from A) OM and B) SEM analyses.

1437 cm^{-1} (CH_2 bending), 1336 cm^{-1} (CH_x bending, C-O-H bending), 1247 cm^{-1} (C-O-H bending), 1150 cm^{-1} (C-O stretching, C-O-H bending, C-C stretching), 1076 cm^{-1} and 995 cm^{-1} (C-O stretching, C-O-H bending, C-C stretching), 931 cm^{-1} (skeletal mode involving the beta C-O-C linkage), 861 cm^{-1} (CH_x bending), and 761 cm^{-1} (skeletal mode involving the beta C-O-C linkage).

Cyclamen sp., *Cyperus rotundus*, *Erythronium dens-canis*, *Heracleum sibiricum*, *Pastinaca sativa*, *Quercus ilex*, and *Sagittaria sagittifolia*, show similar FTIR spectra to the one of *Solanum tuberosum* (Fig. S6; S7; S10; S11; S17; S20; S22), thus the identified characteristic IR absorption bands are mainly related to amylose and amylopectin.

The other starches extracted showed some meaningful differences with respect to *Solanum tuberosum*. In particular, for starches extracted from *Arundo donax*, *Cannabis sativa, Iris sibirica; Oxalis acetosella*, *Paeonia officinalis*, *Pisum sativum, Rumex acetosa, Sorghum halepense*, *Triticum dicoccum*, and *Zea mays* (Fig. S1; S3; S12; S16; S18; S19; S21; S23; S26; S27), an increase in the intensity signal at around 1640 cm^{-1} and the appearance of a new band at around 1530 cm^{-1} were registered, which could be assigned to Amide I and Amide II bands, respectively, from proteins. This latter band was less intense in *Iris sibirica*, *Triticum dicoccum*, and *Zea mays.*

Another group of starches, extracted from *Avena sativa*, *Carex humilis*, *Castanea sativa*, *Convallaria majalis*, *Echinocloa crus-galli*, *Linum usitatissimum*, and *Typha latifolia* (Fig. S2; S4; S5; S8; S9; S15; S24), in addition to the bands at around 1640 and 1530 cm^{-1} (Amide I/II), also showed a small band at 1745 cm^{-1}, corresponding to C=O stretching. As reported by Martínez-Sanz et al. (2018), the presence of these bands at around 1740 cm^{-1} and 1540 cm^{-1}, can be attributable to un-conjugated ketones, esters and acetyl groups from macro-molecules such as hemicelluloses, lignin and pectin that have been extracted in water together with the starches, but also from proteins and carboxylic acids (i.e., fatty acids) included in starches (Wang et al., 2020).

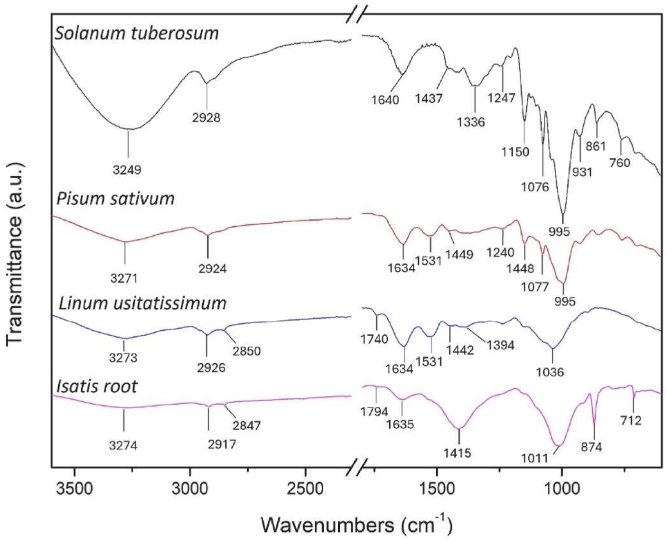

Fig. 7. FTIR spectra of selected starches in the region 3600 - 600 cm^{-1}.

Finally, *Isatis tinctoria* starches from the root show a small band at approximately 1790 cm^{-1}, a broad and intense band at around 1400 cm^{-1} and two narrow bands at 874 and 712 cm^{-1}, probably due to the presence of calcite ($CaCO_3$) (Zhang et al., 2018). These signals are also present in the *Isatis tinctoria* starches from the leaf, but they are less intense (Figures S13-S14).

3.4. Fatty acids characterization by GC-MS analysis

Fatty acids (FAs) are not structural components of starch itself, but rather molecules that are intrinsically associated with and often encapsulated within starch granules during their biosynthesis. This occurs particularly by forming amylose-lipid complexes (V-type complexes), an association crucial to many of starch's properties (Jane et al., 1999; Hoover, 2001). Key characteristics such as crystallinity, gelatinization behavior, and interactions with other biomolecules are dictated by these factors (Gallant et al., 1997). Indeed, due to their chemical and thermal stability, and hydrophobicity, these FAs associated with starch granules persist in situ for extended periods (Whelton et al., 2021). This makes them valuable biomarkers for identifying original plants or plant groups, providing crucial insights into plant sources, processing methods (e.g., thermal treatments), and their preservation state (i.e., integrity of FAs; Dudd et al., 1998; Evershed, 2008; García-Granero et al., 2022; Ordoñez-Araque et al., 2024). Despite the fact that analytical techniques used to analyze FAs (e.g., GC-MS) require only minute sample amounts, the availability of such quantities in archaeological contexts is often limited. This challenge is further compounded by the lack of a systematic study on the quantity and profile of FAs associated with starches derived from plants not of commercial interest. Addressing this gap by creating a reference collection of FA types and quantities in starches from various non-commercial plants could represent a significant step forward in broadening our understanding of plant biomarkers in archaeological contexts. With the aim of identifying FA profiles that could be used to associate starches with their botanical source, we detected the presence of both saturated and unsaturated FAs on starch grains by GC-MS. Fig. 8 illustrates the abundance (expressed in μg/mg) of the predominant FAs identified in the starches extracted from the plants selected for this research. The overall data are reported in Table S2 and examples of GC-MS total ion chromatograms (TICs) are available in Fig. S32. Across nearly all samples, saturated long-chain monofatty acids (predominantly, myristic, palmitic, and stearic), saturated difatty acids (mainly azelaic and sebacic), and unsaturated mono-FAs (palmitoleic, oleic, linoleic, and linolenic) were identified.

GC-MS data (Fig. 8) reveal significant variability of FA content in starches across the different plant species analyzed. In particular, *Cannabis sativa*, *Heracleum sibiricum*, *Paeonia officinalis*, *Pisum sativum*, *Erythronium dens-canis*, and *Sagittaria sagittifolia* exhibited the highest FA concentrations (all >100 μg/mg, listed in decreasing order of abundance). Conversely, *Cyperus rotundus*, *Rumex acetosa*, *Triticum dicoccum*, *Sorghum halepense*, and *Carex humilis* contained the lowest amounts (all <5 μg/mg, also presented in decreasing order of abundance).

Saturated and unsaturated FAs vary by species and processing methods. In general, the most abundant FAs detected in the starches analyzed were palmitic, oleic, and linoleic acid. Similar findings have been reported in the literature regarding the FAs commonly found in cereals (Morrison, 1988; Pastor et al., 2020; Mansouri et al., 2021). Minor components frequently include stearic, myristic, and linolenic acids. These profiles reflect both genetic and environmental influences on lipid composition (Schmid and Ohlrogge, 2008). Oleic acid was also detected in most samples, with exceptions in *Oxalis acetosella*, *Solanum tuberosum*, and *Zea mays*, and only in low amounts (<0.1 μg/mg) in *Cyclamen* sp., *Isatis tinctoria*, *Convallaria majalis*, and *Heracleum sibiricum.*

Among the analyzed starches, those from *Cannabis sativa* exhibited the highest overall concentration of FAs, with oleic and palmitic acids being predominant. Similarly, *Linum usitatissimum* starches showed a notably high abundance of oleic acid. Other species, including *Erythronium dens-canis*, *Heracleum sibiricum*, *Paeonia officinalis*, *Pisum sativum*, and *Sagittaria sagittifolia*, displayed elevated levels of palmitic and linoleic acids in their starches. Myristic acid was generally present in low concentrations across most samples; however, comparatively higher levels were observed in *Heracleum sibiricum*, *Paeonia officinalis*, *Sagittaria sagittifolia*, and, to a lesser extent, in *Pisum sativum*.

Furthermore, it is notable that a group of acids, including lauric, azelaic, sebacic, palmitoleic, and linolenic acids is absent or present in trace quantities (<0.1 μg/mg) in the starch of some species, such as *Avena sativa, Cannabis sativa, Castanea sativa, Linum usitatissimum*, *Carex humilis*, *Echinocloa crus-galli, Oxalis acetosella, Solanum tuberosum,* and *Triticum dicoccum.*

Starch samples from two distinct organs of *Isatis tinctoria*—leaves and roots—were analyzed in this study. It is noteworthy that the FA profiles obtained from both plant parts exhibited a high degree of similarity, demonstrating the reproducibility and reliability of the analytical method employed as reported in previous studies on plant lipidomics (Schmid and Ohlrogge, 2008; Shuman et al., 2010; Hill and Roessner, 2013). Consistently, the GC–MS TICs of root and leaf extracts (Fig. 9a, b) show the same dominant peaks at comparable retention times (e.g., peaks 1–3 and 6, alongside the internal standard), confirming a largely conserved qualitative profile across organs. Notably, the leaf TIC exhibits additional unsaturated FA methyl esters signals (peaks 4–5) and a higher relative intensity of the palmitate-derived signal (peak 2) compared with the root TIC, in which peaks 4–5 are not evident. More significantly, these findings suggest that starch extracted from different organs of the same species may have comparable FA compositions, with the notable exception of palmitic acid, which was observed at slightly higher concentrations in leaf-derived starch relative to root-derived starch. This organ-specific variation in palmitic acid content aligns with previous reports of differential lipid distribution across plant tissues (Lytovchenko et al., 2009; Napier et al., 2014), thus reflecting distinct physiological roles or metabolic activities associated with starch biosynthesis and storage in leaves compared to roots.

Cluster analysis of the complete dataset revealed two principal groups, highlighted by red and black rectangles (Fig. 10). In addition to the trends previously discussed, samples within the red cluster are characterized by high concentrations of linoleic acid (>55 μg/mg) and palmitic acid (>50 μg/mg). Conversely, samples within the black rectangle generally exhibit low levels of both linoleic acid (<20 μg/mg) and palmitic acid (<8 μg/mg), with *Cannabis sativa* representing a notable exception. Additionally, the violet rectangle identifies the two samples with exceptionally high concentrations of oleic acid.

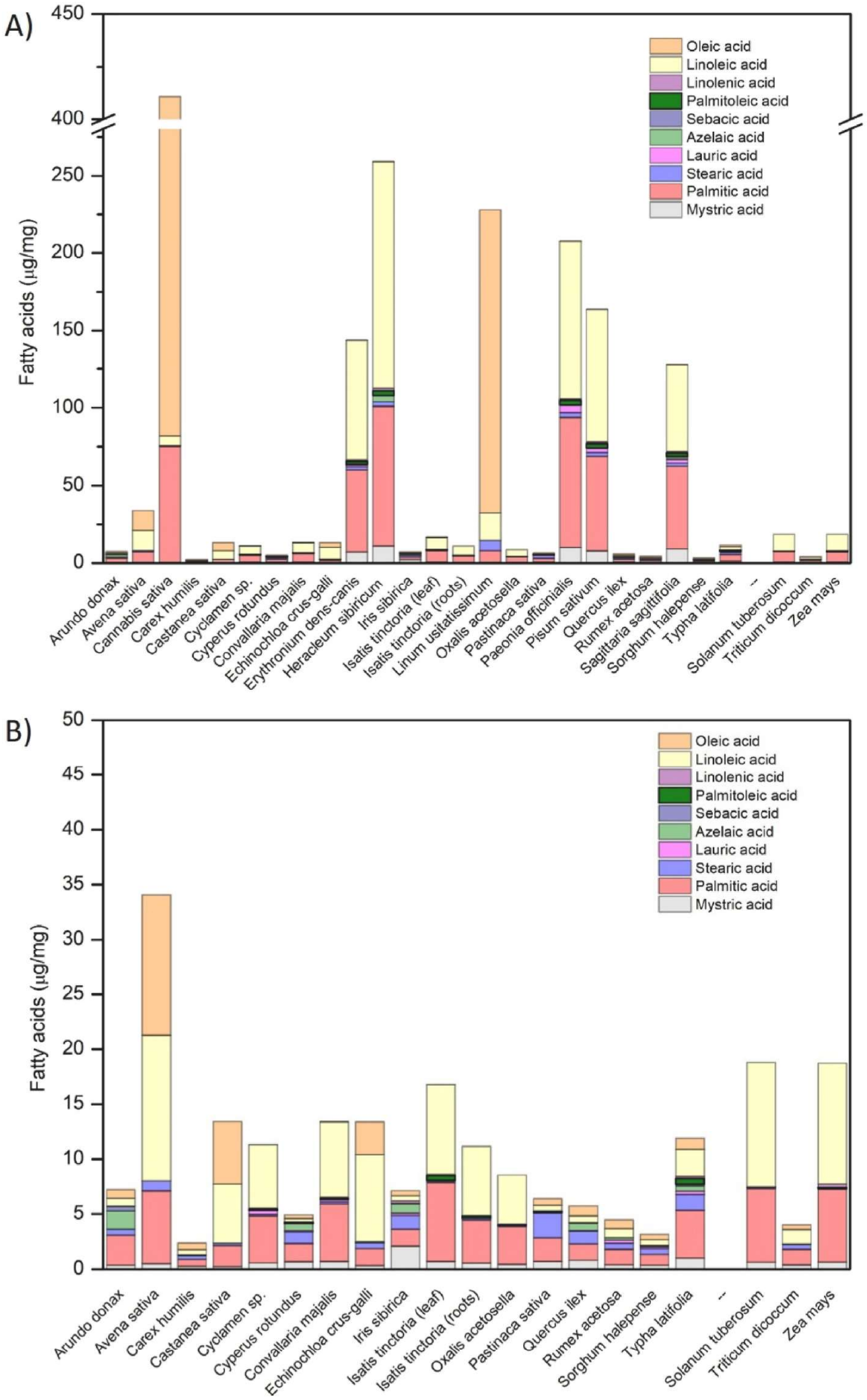

Fig. 8. Quantification of fatty acids (expressed in µg/mg) detected by GC-MS in starches considered in this study. A: Histograms showing all analyzed samples. B: Focus on samples with fatty acid concentrations equal to or above 50 µg/mg.

Although the hierarchical clustering did not reveal a significant pattern, such as the grouping of plant families by FA type and concentration, GC–MS results may still be helpful in providing complementary information to other techniques (i.e., OM, SEM, FTIR, Time-of-Flight Secondary Ion Mass Spectrometry) used for plant identification in archaeological contexts (Longo et al., 2021).

In addition, although linoleic and linolenic acids are common constituents of modern plant lipids and reference starches, their direct preservation in archaeological contexts is rare due to their high susceptibility to oxidative degradation. In archaeological samples, these polyunsaturated FAs are therefore generally absent or occur only as trace components, as discussed by Whelton et al. (2021). Consequently, FA profiles obtained by GC–MS should not be interpreted as direct equivalents of modern reference materials, but rather in terms of degradation pathways and the presence of more stable oxidation products derived from unsaturated precursors.

The identification of azelaic and sebacic acids is consistent with the oxidative degradation of unsaturated FAs originally present in plant-

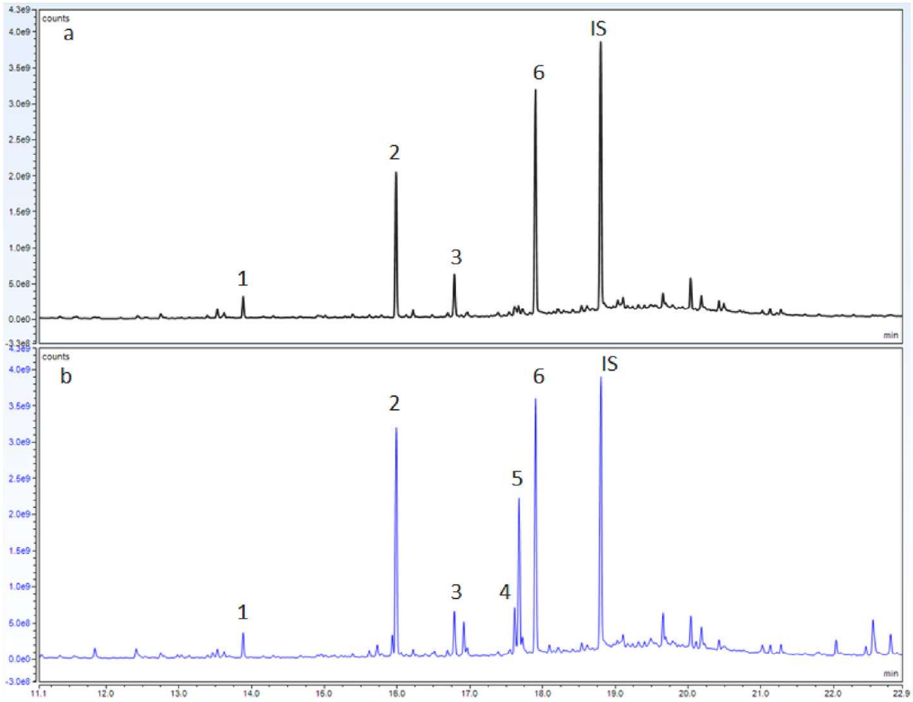

Fig. 9. GC–MS total ion chromatograms (TICs) of *Isatis tinctoria* extracts: (a) root and (b) leaf. Major peaks were assigned as follows: 1, myristic acid methyl ester (methyl myristate); 2, palmitic acid methyl ester (methyl palmitate); 3, N-methylbenzenesulfonanilide (indigo-related compound detected in both root and leaf); 4, linoleic acid methyl ester (methyl linoleate); 5, linolenic acid methyl ester (methyl linolenate); 6, stearic acid methyl ester (methyl stearate). IS, internal standard (nonadecanoic acid).

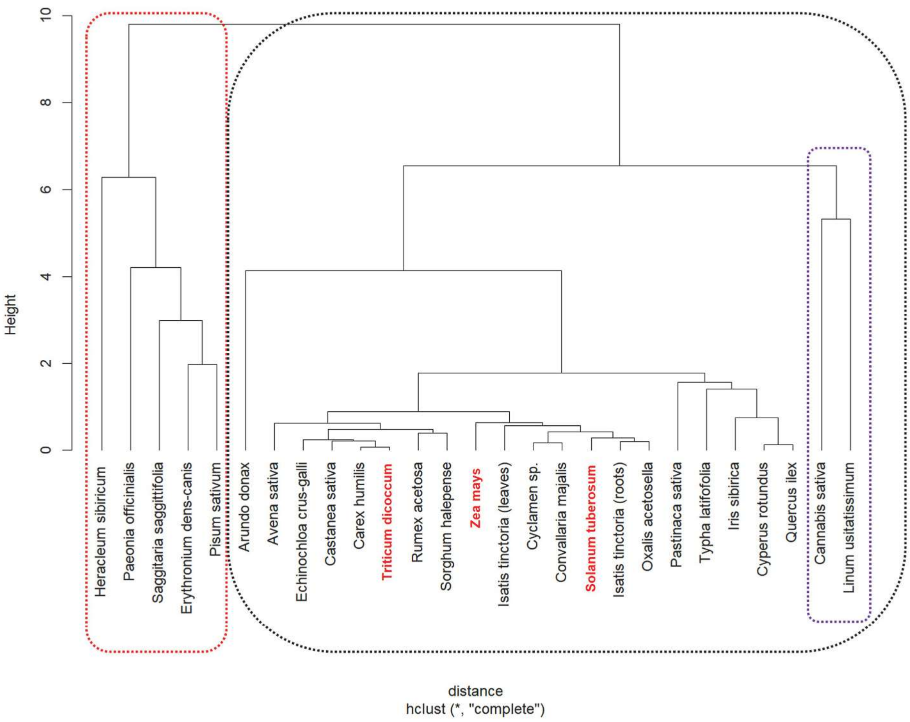

Fig. 10. Hierarchical cluster analysis of fatty acid profiles in extracted starches. In red are shown the 3 non-Eurasian taxa. (For interpretation of the references to color in this figure legend, the reader is referred to the Web version of this article.)

derived lipids. These compounds are commonly reported as the dominant dicarboxylic acids in degraded lipid assemblages, while suberic acid—although theoretically expected to co-occur—is often present only in minor amounts and may fall below detection limits in archaeological samples. Experimental and heritage science studies have shown that such dicarboxylic acid distributions reflect advanced oxidation processes affecting polyunsaturated FAs, particularly linoleic and linolenic acids (e.g. Izzo et al., 2014; Fuster-López et al., 2019).

In our case, the use of GC-MS was not feasible for the archaeological samples due to the extremely limited amount of material and the destructive nature of the technique, which poses clear constraints when dealing with unique archaeological specimens. Instead, the GC-MS reference data were used to support the identification of specific FTIR signals as FAs.

3.5. Comparison with archaeological samples

Analysis of archaeological starches, obtained via sonication in water from molds of GSTs BZ442 and BZ833 from Brînzeni I (Longo et al., 2021, 2022; Birarda et al., 2023), was conducted by means of OM, SEM and FTIR (Figs. 11 and 12). OM and SEM provide complementary information: OM confirms starch through the presence of the Maltese cross, while both techniques allow detailed observations on granule morphology, preservation, and potential mechanical or thermal alteration. FTIR further strengthens starch identification through characteristic amylose and amylopectin absorption bands, particularly when the Maltese cross is obscured by sediment or when the granule is degraded. It can also detect functional groups that indicate diagenetic processes, confirming the starch's ancient origin. In the analyzed samples, OM clearly showed starch grains with a damaged Maltese cross (Fig. 11A and B and D-E). Moreover, a clear fracture was seen in the grain from sample BZ442 (Fig. 11A and B), while the starch grain from BZ833 presented a central depression, a feature often associated with exposure to heat (Fig. 11D and E). The microphotographs acquired at the SEM show two different starch grains; the first seemingly presents adhering soil (Fig. 11C), while the other shows a flaked surface, likely the result of fractured lamella (Fig. 11F). The use of synchrotron radiation was crucial to perform FTIR analysis as it permitted single starch grain investigation (Birarda et al., 2023). Conventional FTIR requires substantially larger sample quantities, which are typically unavailable for archaeological material of this chronology, and it does not allow single-grain measurements, which are essential when samples may contain starches originating from different plant sources. Subsequently, a comparative analysis of modern and archaeological spectra was performed to ascertain whether features observed in modern starches could indicate the botanical source or organ of origin of these ancient starches.

FTIR imaging (Fig. 12A–C) allowed for the morphological inspection of the mineral and organic residues deposited on the ZnSe window. Then, according to the procedure described in Birarda et al. (2023), FTIR analysis (Fig. 12 D) was performed on the five points marked in Fig. 12A-B-C. FTIR imaging revealed that grains BZ442_#2, BZ442_#3 and BZ442_#4 were quite well isolated and clean, while grains BZ442_#1 and BZ833_#1 had a lot of adhered material. The spectra presented in Fig. 12D confirm their identification as starches, as most of the characteristic peaks observed in modern ones were present. Specifically, bands between 3600 and 3000 cm^{-1} and at 1630 cm^{-1} are attributed to -OH stretching and bending vibrations, respectively. A band between 3000 and 2800 cm^{-1} corresponds to C-H stretching, and the main bands in fingerprint region (1200-900 cm^{-1}) are as previously described.

The broad O-H stretching band, typically centered ~3450 cm^{-1} region, shifts to approximately 3300 cm^{-1} in all the archaeological samples and often it is paired with a sharp band at 3610 cm^{-1} due to free -OH and weakly bonded -OH (Palchowdhury et al., 2022). The band shift and the extra peak may be attributed to varying states of order, likely a consequence of aging (Gallina et al., 2006). With regards to grains BZ442_#1 and BZ833_#1 and compared to the other archaeological examples, they exhibited better preserved spectral characteristics with well-defined peaks. Conversely, the spectra of grains BZ442_#2 and BZ442_#4 showed broad, poorly defined bands at 1020 cm^{-1}, weak signals of the CH_2 in the 2800-3000 cm^{-1} range and a weak, broad band of OH stretching at ~3300 cm^{-1}. This suggests a disordered starch structure, the presence of minor organic compounds/contaminants (possibly from other plant matter), or environmental degradation products and high levels of degradation and dehydration. Finally, the spectrum of grain BZ833_#1, even though well preserved, displayed a broad band at 1430 cm^{-1} and two smaller signals at 1780 and 2511 cm^{-1} that could be linked to carbonate signals and may be related to the starch's partial mineralization, as previously observed (Birarda et al., 2023).

The presence of a very weak peak at 1733 cm^{-1} in BZ833_#1, one of the better-preserved particles, can be attributed to the presence of a minor component of FAs that can contribute to the long-term preservation of the starch grains.

Based on the results obtained, all the analyzed particles are confirmed to be starch grains. Some specimens, however, could not be assigned to a specific taxon because their optical characteristics were too heavily degraded for reliable identification. Notably, these same

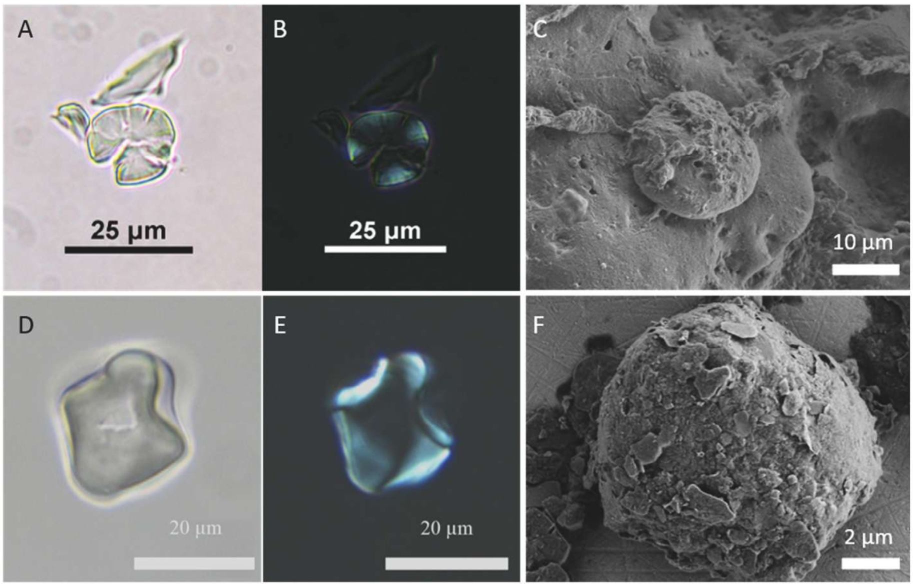

Fig. 11. Micrographs of archaeological starches from Brînzeni I GSTs BZ442 (A-C) and BZ833 (D-F). The starch grains viewed under OM in brightfield and polarized light (two left columns) and those observed at SEM (right column) are not the same.

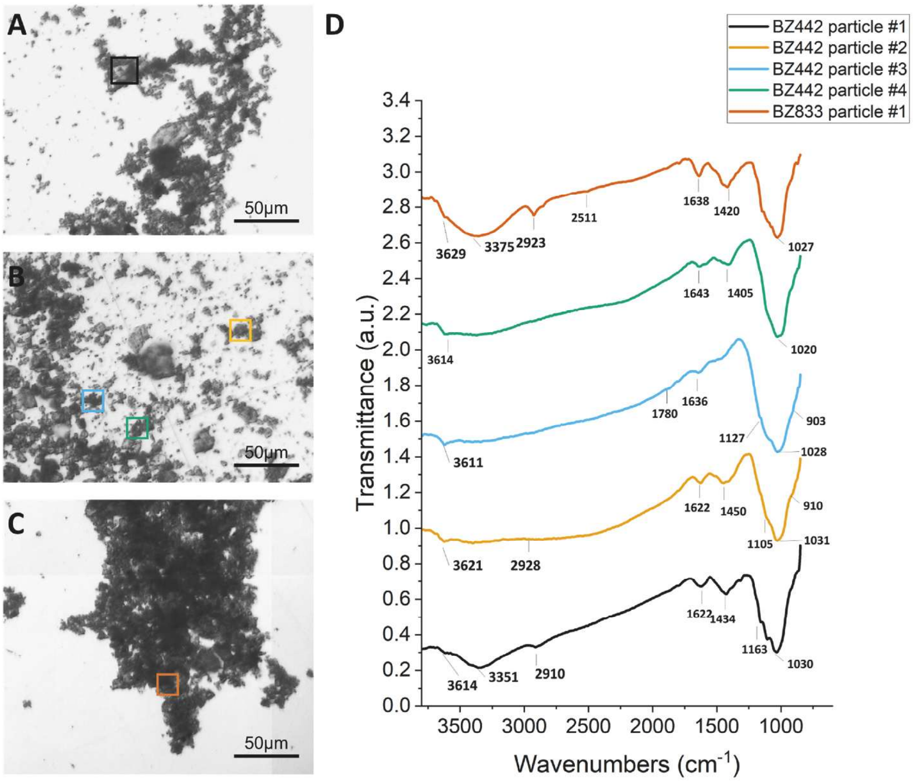

Fig. 12. Analysis of five potential starch grains from archaeological contexts. A-B) Optical images of the sample obtained from BZ442 with four particles identified as potential starches and C) of one particle obtained from sample BZ833; D) FTIR spectra of the selected potential starches in the region 3800 - 800 cm^{-1}.

damages may provide important information on how these plants could have been treated or processed in the past. The starch grains observed using SEM are more identifiable, given their more intact state. Based on a comparison with imaging data from our reference collection, and supported by morphometric information from granulometric analyses of the modern reference material, we can infer that one grain (Fig. 11C) could belong to the Triticeae tribe in the Poaceae (grass) family, while the second (Fig. 11F), is similar to starches produced by *Sorghum halepense*. FTIR analysis confirms that the selected spots show the typical amylose and amylopectin signals and possibly the presence of FAs (signals at 1730 cm^{-1}) and proteins (amides in the region 1640 - 1530 cm^{-1}). In this framework, GC-MS—used on modern starches to investigate their content—was not applied to the archaeological samples. Owing to the destructive nature of the technique and the extremely limited quantity of archaeological material available, GC–MS was deemed unsuitable, despite requiring only very small sample volumes. Consequently, GC–MS results from modern starches were primarily used to support the interpretation of FTIR spectra rather than to analyze the archaeological samples directly. This decision does not diminish GC–MS's value in archaeological research. On the contrary, it can provide highly informative data when applied to appropriate proxy materials, and it should be considered whenever the technique can yield relevant and diagnostic results. When sample availability permits, GC-MS remains a powerful tool for characterizing organic residues.

Our study highlights the necessity of a multi-technique analytical approach, as no single method can consistently provide all the information required to confidently identify starches and contribute to archaeological interpretation. This approach, however, presents an inherent challenge: it is often difficult to analyze the same area—or even the same starch granule—using multiple techniques. Moreover, it is not always possible to apply destructive methods without risking the loss of rare and irreplaceable archaeological material. For these reasons, analytical strategies that rely on proxy materials and prioritize non-destructive techniques are strongly recommended, as they maximize the information that can be obtained from precious archaeological samples. In addition, future methodological advances that allow samples to be marked and repeatedly analyzed in exactly the same area would significantly enhance the reliability and comparability of multi-technique analytical approaches.

4. Conclusions

Starch analysis has the potential to be a highly informative tool, given its ability to withstand thousands of years in archaeological contexts (i.e., lithic and ceramic artifacts, dental calculus, coprolites). Starch grains offer unique insight into past human activities and the use of perishable materials, as well as subsistence practices such as the preparation and processing of plant-based resources, and interactions with the environment, including the use of specific plant taxa. Despite this potential, the application of starch grain analysis in archaeology is constrained by several significant challenges. These include issues related to the state of preservation of starch grains over time, which alter their morphology, and biases inherent in extraction and identification techniques. Moreover, there is a lack of comprehensive reference collections, particularly for wild or non-domesticated plants that were likely significant in the Paleolithic but are not economically relevant today and are therefore not easily accessible.

This study addresses two of these limitations. First, it contributes a novel multi-technique reference collection of 23 starches derived from plants likely to have existed during MIS 3 and from 3 non-Eurasian taxa. While the collection is not yet exhaustive—although a significant effort to expand the collection is ongoing—this work represents a critical first step in characterizing a range of plant families and plant organs, allowing researchers to more confidently distinguish ancient starches and differentiate them from potential modern contaminants. Secondly, the approach adopted here goes beyond traditional morphology-based identification. While shape and size remain valuable diagnostic features, they are often compromised in archaeological samples due to diagenetic processes, including enzymatic attacks or intentional human activities such as mechanical alteration (i.e., grinding and pounding of plant organs) or exposure to heat. By integrating chemoprofiling techniques, this study demonstrates that chemical composition can serve as a complementary analysis to confirm the presence of starch, even if the grains are altered by the aforementioned processes. Moreover, these techniques facilitate the identification of starch grains even when they are embedded in complex matrices such as soil, and could also be successfully applied to dental calculus or coprolites, contexts in which the isolation of elements for microscopic analysis is often challenging. Indeed, the integration of FTIR analysis of archaeological samples, compared against our modern starch reference collection, was key in confirming the starch nature of the observed features. The analysis of spectral signatures also revealed specific signals that can be linked to age-related degradation, mineralization or processing effects. This is also evident from the microscopy analysis. Indeed, images showed damage to the Maltese cross and to the overall morphology of the grains.

While GC-MS offers significant insights into starch architecture and composition through fatty acid profiling, particularly in non-commercial botanical sources, its application to archaeobotanical specimens presents considerable methodological challenges. The limitation in the quantities of starch commonly encountered in archaeological contexts could make GC-MS analysis operationally unfeasible. However, the spectroscopic detection of an IR absorption band at approximately 1740 cm^{-1} provided a non-specific indicator on the presence of an esterified FA.

This study also highlights some limitations of current analytical procedures. The most evident one is surely the impossibility of performing all the aforementioned analyses on the same archaeological starch granule. Moving the sample from one instrument to another can result in the loss of a reference coordinate, and in turn, can lead to a reduction in the probability of identifying the same areas of interest. Moreover, the different procedures for sample observation (i.e., wet vs. dry; with or without a coverslip; type of support for sample deposition) introduce an additional hurdle to the analytical sequence.

Overall, this approach offers a more robust analytical framework that can enhance the reliability of identifications, even in cases where starch grains are poorly preserved or altered, and help distinguish between ancient and modern unaltered contaminants.

Data availability statement

All raw data supporting the findings of this study are available in Supplementary Information.

Funding

This work was supported by NTU (Singapore) SUG grant M4081669.090 (LL), UniCampania, Visiting Professor, 2018 to LL, hosted at DiSTABIF by C. Lubritto. Part of the study was funded through the ANR project Starch4Sapiens (AAPG2020 CE03-0002) coordinated by SC (CNRS-AMU, Marseille, France) (SC, AC, LL, CC, EB). Additional funding was provided by the Italian Ministry of University and Research (MUR) PRIN-2022 2022XX8BRT "Reversible absorbent smart materials for molecular archaeology to disclose Palaeolithic stone tools as bio-archives-SMarT4BioArCH", financed by European Union - Next Generation EU, Mission 4, Component 1, CUP Master & CUP B53DZ3014020006 (EB, GS).

CRediT authorship contribution statement

C. Cagnato: Data curation, Investigation, Visualization, Writing – original draft, Writing – review & editing. **G. Sorrentino:** Data curation, Investigation, Visualization, Writing – original draft, Writing – review & editing. **A. Bonetto:** Formal analysis, Investigation, Resources, Writing – review & editing. **F.C. Izzo:** Formal analysis, Investigation, Resources, Writing – original draft, Writing – review & editing. **A. Brunelli:** Data curation, Formal analysis, Investigation, Visualization, Writing – review & editing. **G. Birarda:** Formal analysis, Investigation, Resources, Visualization, Writing – review & editing. **L. Vaccari:** Investigation, Resources, Writing – review & editing. **S. Condemi:** Funding acquisition, Project administration, Supervision, Writing – review & editing. **A. Carbone:** Project administration, Resources, Writing – review & editing. **A. Marcomini:** Resources, Supervision, Writing – review & editing. **L. Longo:** Conceptualization, Funding acquisition, Investigation, Methodology, Resources, Writing – original draft, Writing – review & editing. **E. Badetti:** Conceptualization, Data curation, Formal analysis, Funding acquisition, Investigation, Methodology, Project administration, Resources, Supervision, Visualization, Writing – original draft, Writing – review & editing.

Declaration of competing interest

The authors declare that they have no known competing financial interests or personal relationships that could have appeared to influence the work reported in this paper.

Acknowledgments

General: We are thankful to D. Zanini, Scientific Coordinator of the *Orto Botanico di Novezzina* (Monte Baldo, Verona) and to K. Cianfaglione, Université Catholique de Lille, France; to R. Ciancio and S. Dal Zilio for the access to the SEM facilities accessed at IOM-CNR, Trieste, Italy; to G. Lusvardi SEM facility at University MoRe (Modena and Reggio, Italy). CC is grateful to *MSH Mondes* in Nanterre and IBPS/Institut de Biologie Paris-Seine of the Sorbonne Université/CNRS (Paris, France) where the OM and SEM observations were carried out. We also would like to acknowledge Irina Pantyukhina for photos of archaeological starch grains from Brînzeni. We finally acknowledge Michaël Trichet from the IBPS electron microscopy core facility and the support of « Région Île-de-France », Sorbonne-Université and the CNRS.

Appendix A. Supplementary data

Supplementary data to this article can be found online at https://doi.org/10.1016/j.jas.2026.106570.

References

Adovasio, J.M., Soffer, O., Klíma, B., 1996. Upper Palaeolithic fibre technology: interlaced woven finds from Pavlov I, Czech Republic, c. 26,000 years ago. Antiquity 70 (269), 526–534. https://doi.org/10.1017/S0003598X0008368X.

Ahituv, H., Henry, A.G., Melamed, Y., Goren-Inbar, N., Bakels, C., Shumilovskikh, L., et al., 2024. Starch-rich plant foods 780,000 y ago: evidence from Acheulian percussive stone tools. Proc. Natl. Acad. Sci. U. S. A 122 (3), e2418661121. https://doi.org/10.1073/pnas.2418661121.

Ahituv, H., Henry, A.G., 2022. An initial key of starch grains from edible plants of the Eastern mediterranean for use in identifying archaeological starches. J. Archaeol. Sci.: Report 42, 103396. https://doi.org/10.1016/j.jasrep.2022.103396.

Allsworth-Jones, P., Borziac, I.A., Chetraru, N.A., French, C.A.I., Medyanik, S.I., 2018. Brînzeni: a multidisciplinary study of an upper Palaeolithic site in Moldova. Proc. Prehist. Soc. 84, 41–76.

Ameur, A., Enroth, S., Johansson, Å., Zaboli, G., Igl, W., Johansson, A.C.V., Rivas, M.A., Daly, M.J., 2012. Genetic adaptation of fatty-acid metabolism: a human-specific haplotype increasing the biosynthesis of long-chain Omega-3 and Omega-6 fatty acids. Am. J. Hum. Genet. 90, 809–820.

Aranguren, B., Longo, L., Mariotti Lippi, M., Revedin, A., 2011. Evidence of edible plant exploitation. Pavlov excavations 2007- 2011. The Dolni Vĕstonice Studies 8, 170–179.

Barton, H., Mutri, G., Hill, E., Farr, L., Barker, G., 2018. Use of grass seed resources c.31 ka by modern humans at the Haua Fteah cave, Northeast Libya. J. Archaeol. Sci. 99, 99–111.

Becker, R.A., Chambers, J.M., Wilks, A.R., 1988. The New S Language. Wadsworth & Brooks/Cole (S version.).

Bestel, S., Crawford, G.W., Liu, L., Shi, J., Song, Y., Chen, X., 2014. The evolution of millet domestication, middle yellow river region, North China: evidence from charred seeds at the late Upper Paleolithic Shizitan Locality 9 site. Holocene 24 (3), 261–265. https://doi.org/10.1177/0959683613518595.

Bigga, G., Schoch, W., Urban, B., 2015. Paleoenvironment and possibilities of plant exploitation in the middle Pleistocene of Schöningen (Germany). Insights from botanical macro-remains and pollen. J. Hum. Evol. 89, 92–104. https://doi.org/10.1016/j.jhevol.2015.10.005.

Birarda, G., Badetti, E., Cagnato, C., Sorrentino, G., Pantyukhina, I., Stani, C., et al., 2023. Morpho-chemical characterization of individual ancient starches retrieved on ground stone tools from Palaeolithic sites in the pontic steppe. Sci. Rep. 13, 21713. https://doi.org/10.1038/s41598-023-46970-8.

Birarda, G., Bedolla, D., Piccirilli, F., Stani, C., Vondracek, H., Vaccari, L., 2022. Chemical analyses at micro and nano scale at SISSI-Bio beamline at Elettra-Sincrotrone Trieste. Biomedical Vibrational Spectroscopy 2022: Advances in Research and Industry 11957, 27–39.

Blinnikov, M.S., Gaglioti, B.V., Walker, D.A., Wooller, M.J., Zazula, G.D., 2011. Pleistocene graminoid-dominated ecosystems in the Arctic. Quat. Sci. Rev. 30, 2906–2929. https://doi.org/10.1016/j.quascirev.2011.07.002.

Boeskorov, G.G., Bakulina, N.T., Davydov, S.P., Shchelchkova, M.V., Solomonov, N.G., 2011. Study of pollen and spores from the stomach of a fossil woolly rhinoceros found in the lower reaches of the Kolyma river. Dokl. Biol. Sci. 436 (1), 23. https://doi.org/10.1134/S0012496611010017.

Bresch, H., Hodoroaba, V.D., Schmidt, A., Rasmussen, K., Rauscher, H., 2022. Counting small particles in electron microscopy images—proposal for rules and their application in practice. Nanomaterials 12 (13), 2238. https://doi.org/10.3390/nano12132238.

Cagnato, C., Hamon, C., Salavert, A., Elliott, M., 2021. Developing a reference collection for starch grain analysis in early Neolithic Western temperate Europe. Open Archaeol. 7 (1), 1035–1053. https://doi.org/10.1515/opar-2020-0186.

Cagnato, C., Ponce, J.M., 2017. Ancient Maya manioc (Manihot esculenta Crantz) consumption: starch grain evidence from late to terminal classic (8th–9th century CE) occupation at La Corona, northwestern Petén, Guatemala. J. Archaeol. Sci.: Report 16, 276–286. https://doi.org/10.1016/j.jasrep.2017.09.035.

Calder, P.C., 2015. Functional roles of fatty acids and their effects on human health. Journal of Parenteral and EnteralNutrition 39 (1), 18S–32S. https://doi.org/10.1177/0148607115595980.

Calzolari, F., 2026. Il viaggio di monte Baldo della magnifica città di Verona. Digitized in2013. Accessed from. https://books.google.it/books/about/Il_viaggio_di_monte_Baldo_della_magnific.html?id=G3lVAAAAcAAJ&redir_esc=y.

Caravá, S., García, C.R., de Agredos-Pascual, M.L.V., Mascarós, S.M., Izzo, F.C., 2020. Investigation of modern oil paints through a physico-chemical integrated approach. Emblematic cases from Valencia, Spain. Spectrochim. Acta Mol. Biomol. Spectrosc. 240, 118633. https://doi.org/10.1016/j.saa.2020.118633.

Carbone, A., Longo, L., Condemi, S., 2025. Dans le ventre de l'évolution humaine. Histoire de la recherche contemporaine, tome XIII N.2.

Copeland, L., Hardy, K., 2018. Archaeological starch. Agronomy 8 (1), 4. https://doi.org/10.3390/agronomy8010004.

Cortella, A.R., Pochettino, M.L., 1994. Starch grain analysis as a microscopic diagnostic feature in the identification of plant material. Econ. Bot. 48 (2), 171–181.

Crowther, A., 2009. Morphometric analysis of calcium oxalate raphides and assessment of their taxonomic value for archaeological microfossil studies. In: Archaeological Science Under a Microscope: Studies in Residue and Ancient DNA Analysis in Honour of Thomas H. Loy, vol. 30, pp. 102–128.

Daniau, Anne-Laure, Desprat, Stéphanie, Aleman, Julie C., Bremond, Laurent, Davis, Basil, et al., 2019. Terrestrial plant microfossils in palaeoenvironmental studies, pollen, microcharcoal and phytolith. Towards a comprehensive understanding of vegetation, fire and climate changes over the past one million years. Revue de Micropaléontologie 63, 1–35. https://doi.org/10.1016/j.revmic.2019.02.001. https://linkinghub.elsevier.com/retrieve/pii/S0035159818300667.

Deka, G., Gautam, G., Duarah, A., Roy, A., Dutta, H., 2024. Analytical tools for starch characterization. In: Mazumder, N., Rahman, M.H. (Eds.), Advanced Research in Starch. Springer, Singapore. https://doi.org/10.1007/978-981-99-9527-1_8.

Dhital, S., Brennan, C., Gidley, M.J., 2019. Location and interactions of starches in planta: effects on food and nutritional functionality. Trends Food Sci. Technol. 93, 158–166. https://doi.org/10.1016/j.tifs.2019.09.011.

Dénes, A., Papp, N., Babai, D., Czúcz, B., Molnár, Z., 2012. Wild plants used for food by Hungarian ethnic groups living in the Carpathian Basin. Acta Soc. Bot. Pol. 81 (4). https://doi.org/10.5586/asbp.2012.040.

Dubreuil, L., Nadel, D., 2015. The development of plant food processing in the levant: insights from use-wear analysis of early Epipalaeolithic ground stone tools. Philos. Trans. R. Soc. B 370, 20140357. https://doi.org/10.1098/rstb.2014.0357.

Dudd, S.N., Regert, M., Evershed, R.P., 1998. Assessing microbial lipid contributions during laboratory degradations of fats and oils and pure triacylglycerols absorbed in ceramic potsherds. Org. Geochem. 29 (5–7), 1345–1354. https://doi.org/10.1016/S0146-6380(98)00093-X.

Esau, K., 1977. Plant Anatomy, third ed. John Wiley & Sons.

Evershed, R.P., 2008. Organic residue analysis in archaeology: the archaeological biomarker revolution. Archaeometry 50 (6), 895–924. https://doi.org/10.1111/j.1475-4754.2008.00446.x.

Florin, S.A., Fairbairn, A.S., Nango, M., Djandjomerr, D., Hua, Q., Marwick, B., Reutens, D.C., Fullagar, R., Smith, M., Wallis, L.A., Clarkson, C., 2022. 65,000 years of changing plant food and landscape use at Madjedbebe, Mirarr country, northern Australia. Quat. Sci. Rev. 284, 107498. https://doi.org/10.1016/j.quascirev.2022.107498.

Fuster-López, L., Izzo, F.C., Damato, V., Yusà-Marco, D.J., Zendri, E., 2019. An insight into the mechanical properties of selected commercial oil and alkyd paint films containing cobalt blue. J. Cult. Herit. 35, 225–234. https://doi.org/10.1016/j.culher.2018.12.007.

Gallant, J.D., Bouchet, B., Baldwin, P.M., 1997. Microscopy of starch: evidence of a new level of granule organization. Carbohydr. Polym. 32, 177–191. https://doi.org/10.1016/S0144-8617(97)00008-8.

Gallina, M.E., Sassi, P., Paolantoni, M., Morresi, A., Cataliotti, R.S., 2006. Vibrational analysis of molecular interactions in aqueous glucose solutions. Temperature and concentration effects. J. Phys. Chem. B 110 (17), 8856–8864. https://doi.org/10.1021/jp056213y.

García-Granero, J.J., 2020. Starch taphonomy, equifinality and the importance of context: some notes on the identification of food processing through starch grain analysis. JAS 124. https://doi.org/10.1016/j.jas.2020.105267.

García-Granero, J.J., Suryanarayan, A., Cubas, M., Craig, O.E., Cárdenas, M., Ajithprasad, P., Madella, M., 2022. Integrating lipid and starch grain analyses from pottery vessels to explore prehistoric foodways in Northern Gujarat, India. Front. Ecol. Evol. 10, 840199. https://doi.org/10.3389/fevo.2022.840199.

Gnemmi, M., Fuster-Lòpez, L., Mecklenburg, M., Murray, A., Sands, S., Watson, G., Izzo, F.C., 2024. Ion migration mechanisms in the early stages of drying and degradation of oil paint films. Materials Degradation 8 (1), 63. https://doi.org/10.1038/s41529-024-00472-8.

Goren-Inbar, N., Sharon, G., Melamed, Y., Kislev, M., 2002. Nuts, nut cracking, and pitted stones at Gesher Benot Ya'aqov, Israel. Proc. Natl. Acad. Sci. U. S. A 99 (4), 2455–2460. https://doi.org/10.1073/pnas.032570499.

Gott, B., Barton, H., Samuel, D., Torrence, R., 2006. Biology of starch. In: Ancient Starch Research. Routledge, pp. 35–45.

Hardy, K., 2008. Prehistoric string theory. How twisted fibres helped to shape the world. Antiquity 82 (316), 271–280. https://doi.org/10.1017/S0003598X00096794.

Hardy, B.L., 2010. Climatic variability and plant food distribution in Pleistocene Europe: implications for neanderthal diet and subsistence. Quat. Sci. Rev. 29, 662–679.

Hardy, K., 2018. Plant use in the lower and middle Palaeolithic: food, medicine and raw materials. Quat. Sci. Rev. 191, 393–405. https://doi.org/10.1016/j.quascirev.2018.04.028.

Hardy, B.L., Moncel, M.H., Kerfant, C., et al., 2020. Direct evidence of Neanderthal fibre technology and its cognitive and behavioral implications. Sci. Rep. 10, 4889. https://doi.org/10.1038/s41598-020-61839-w.

Hardy, K., Blakeney, T., Copeland, L., Kirkham, J., Wrangham, R., Collins, M., 2009. Starch granules, dental calculus and new perspectives on ancient diet. J. Archaeol. Sci. 36 (2), 248–255. https://doi.org/10.1016/j.jas.2008.09.015.

Hardy, K., Buckley, S., Copeland, L., 2018. Pleistocene dental calculus: recovering information on Paleolithic food items, medicines, paleoenvironment and microbes. Evol. Anthropol. Issues News Rev. 27 (5), 234–246. https://doi.org/10.1002/evan.21718.

Haslam, M., 2004. The decomposition of starch grains in soils: implications for archaeological residue analyses. J. Archaeol. Sci. 31 (12), 1715–1734. https://doi.org/10.1016/j.jas.2004.05.006.

Hather, J.G., Mason, S.L.R., 2002. Introduction: some issues in the archaeobotany of hunter-gatherers. In: Mason, S.L.R., Hather, J.G. (Eds.), Hunter-Gatherer Archaeobotany: Perspectives from the Northern Temperate Zone: 1–14. Institute of Archaeology, University College London, London.

Hayes, E.H., Fullagar, R., Field, J.H., Coster, A.C.F., Matheson, C., Nango, M., et al., 2022. 65,000-years of continuous grinding stone use at Madjedbebe, Northern Australia. Sci. Rep. 12, 11747. https://doi.org/10.1038/s41598-022-15174-x.

Henry, A.G., 2020. Handbook for the Analysis of Micro-particles in Archaeological Samples. Springer International Publishing, Cham. https://doi.org/10.1007/978-3-030-42622-4.

Henry, A.G., Brooks, A.S., Piperno, D.R., 2014. Plant foods and the dietary ecology of Neanderthals and early modern humans. J. Hum. Evol. 69, 44–54. https://doi.org/10.1016/j.jhevol.2013.12.014.

Hill, C.B., Roessner, U., 2013. Metabolic profiling of plants by GC–MS. In: Weckwerth, W., Kahl, G. (Eds.), The Handbook of Plant Metabolomics, pp. 1–23. https://doi.org/10.1002/9783527669882.ch1.

Hoover, R., 2001. Composition, molecular structure, and physicochemical properties of tuber and root starches: a review. Carbohydr. Polym. 45 (3), 253–267. https://doi.org/10.1016/S0144-8617(00)00260-5.

Hopf, M., Bar-Yosef, O., 1987. Plant remains from hayonim Cave, Western galilee. Paleorient 13–1, 117–120. https://doi.org/10.3406/paleo.1987.4423.

Hurcombe, L.M., 2014. Perishable Material Culture in Prehistory: Investigating the Missing Majority. Routledge.

Ingold, T., 2012. Making culture and weaving the world. In: Matter, Materiality and Modern Culture. Routledge, pp. 50–71.

Iob, A., Botigué, L., 2023. Genomic analysis of emmer wheat shows a complex history with two distinct domestic groups and evidence of differential hybridization with wild emmer from the western fertile Crescent. Veg. Hist. Archaeobotany 32 (5), 545–558. https://doi.org/10.1007/s00334-022-00898-7.

Ivanova, S., Gurova, M., Spassov, N., Hristova, L., Tzankov, N., Popov, V., Marinova, E., Makedonska, J., Smith, V., Ottoni, C., Lewis, M., 2016. Magura Cave, Bulgaria: a multidisciplinary study of Late Pleistocene human palaeoenvironment in the Balkans. Quat. Int. 415, 86–108. https://doi.org/10.1016/j.quaint.2015.11.082.

Izzo, F.C., Rigon, C., Vázquez De Ágredos Pascual, M.L., Campíns-Falcó, P., van Keulen, H., 2022. Life after death: a physicochemical study of materials used by the ancient Maya in human bone ointments. Archaeol. Anthropol. Sci. 14 (1), 7. https://doi.org/10.1007/s12520-021-01473-3.

Izzo, F.C., van den Berg, K.J., van Keulen, H., Ferriani, B., Zendri, E., 2014. 20th century artists' oil paints: the case of the Olii by Lucio Fontana. J. Cult. Herit. 15 (5), 557–563. https://doi.org/10.1016/j.culher.2013.11.003.

Jane, J.L., Chen, Y.Y., Lee, L.F., McPherson, A.E., Wong, K.S., Radosavljevic, M., Kasemsuwan, T., 1999. Effects of amylopectin branch chain length and amylose

content on the gelatinization and pasting properties of starch. Cereal Chem. 76 (5), 629–637. https://doi.org/10.1094/CCHEM.1999.76.5.629.
Kolosova, V., Belichenko, O., Rodionova, A., Melnikov, D., Sõukand, R., 2020. Foraging in boreal forest: wild food plants of the republic of Karelia, NW Russia. Foods 9 (8), 1015. https://doi.org/10.3390/foods9081015.
Kovárník, J., Beneš, J., 2018. Microscopic analysis of starch grains and its applications in the archaeology of the Stone age. Interdiscip. Archaeol 9, 83–93.
Kubiak-Martens, L., 1996. Evidence for possible use of plant foods in Palaeolithic and Mesolithic diet from the site of Całowanie in the central part of the Polish Plain. Veget Hist Archaebot 5, 33–38. https://doi.org/10.1007/BF00189433.
Kuneš, P., Pokorný, P., Šída, P., 2008. Detection of the impact of early Holocene hunter-gatherers on vegetation in the Czech Republic, using multivariate analysis of pollen data. Veg. Hist. Archaeobotany 17 (3), 269–287. https://doi.org/10.1007/s00334-007-0119-5.
Langejans, G.H., 2006. Starch grain analysis on late Iron Age grindstones from South Africa. South. Afr. Humanit. 18 (2), 71–91.
Larbey, C., Mentzer, S.M., Ligouis, B., Wurz, S., Jones, M.K., 2019. Cooked starchy food in hearths ca. 120 kya and 65 kya (MIS 5e and MIS 4) from Klasies River Cave, South Africa. J. Hum. Evol. 131, 210–227. https://doi.org/10.1016/j.jhevol.2019.03.015.
Liu, L., Bestel, S., Shi, J., Song, Y., Chen, X., 2013. Paleolithic human exploitation of plant foods during the last glacial maximum in North China. Proc. Natl. Acad. Sci. USA. 110 (14), 5380–5385. https://doi.org/10.1073/pnas.1217864110.
Longo, L., Altieri, S., Birarda, G., Cagnato, C., Graziani, V., Obada, T., et al., 2021. A multi-dimensional approach to investigate use-related biogenic residues on palaeolithic ground stone tools. Environ. Archaeol. https://doi.org/10.1080/14614103.2021.1975252.
Longo, L., Birarda, G., Cagnato, C., Badetti, E., Covalenco, S., Pantyukhina, I., et al., 2022. Coupling the beams: how controlled extraction methods and FTIR-spectroscopy, OM and SEM reveal the grinding of starchy plants in the Pontic steppe 36,000 years ago. J. Archaeol. Sci.: Report 41, 103333. https://doi.org/10.1016/j.jasrep.2021.103333.
Longo, L., Veronese, M., Cagnato, C., Sorrentino, G., Tetruashvili, A., Belfer-Cohen, A., et al., 2025. Direct evidence for processing Isatis tinctoria L., a non-nutritional plant, 32–34,000 years ago. PLoS One 20 (5), e0321262. https://doi.org/10.1371/journal.pone.0321262.
López-Sáez, J.A., Glais, A., Robles-López, S., et al., 2017. Unraveling the naturalness of sweet chestnut forests (Castanea sativa Mill.) in central Spain. Veg. Hist. Archaeobotany 26, 167–182. https://doi.org/10.1007/s00334-016-0575-x.
Lunn, J., Theobald, H.E., 2006. The health effects of dietary unsaturated fatty acids. Nutr. Bull. 31 (3), 178–224. https://doi.org/10.1111/j.1467-3010.2006.00571.x.
Lytovchenko, A., Beleggia, R., Schauer, N., Isaacson, T., Leuendorf, J.E., Hellmann, H., Rose, J.K., Fernie, A.R., 2009. Application of GC-MS for the detection of lipophilic compounds in diverse plant tissues. Plant Methods 5 (1), 4. https://doi.org/10.1186/1746-4811-5-4.
Ma, Z., Zhang, C., Li, Q., Perry, L., Yang, X., 2017. Understanding the possible contamination of ancient starch residues by adjacent sediments and modern plants in Northern China. Sustainability 9 (5), 752. https://doi.org/10.3390/su9050752.
Madella, M., Jones, M.K., Goldberg, P., Goren, Y., Hovers, E., 2002. The exploitation of plant resources by neanderthals in amud Cave (Israel): the evidence from Phytolith studies. J. Archaeol. Sci. 29 (7), 703–719. https://doi.org/10.1006/jasc.2001.0743.
Magyari, E.K., Kunes, P., Jakab, G., Sümegi, P., Pelánková, B., Schäbitz, F., Braun, M., Chytrý, M., 2014. Late pleniglacial vegetation in eastern-central Europe: are there modern analogues in Siberia? Quat. Sci. Rev. 95, 60–79.
Mansouri, S., Hajji, T., Medimagh, S., Ferchichi, A., 2021. Identification of fatty acid composition by GC-MS analysis of pearled barley flour. Journal of New Sciences 80 (4), 4653–4663.
Mariotti Lippi, M., Aranguren, B., Arrighi, S., Attolini, D., Benazzi, S., Boschin, F., Florindi, S., Moroni, A., Negrino, F., Pallecchi, P., Pisaneschi, L., 2023. New evidence of plant food processing in Italy before 40ka. Quat. Sci. Rev. 312, 108161. https://doi.org/10.1016/j.quascirev.2023.108161.
Mariotti Lippi, M., Foggi, B., Aranguren, B., Ronchitelli, A., Revedin, A., 2015. Multistep Food Plant Processing at Grotta Paglicci (Southern Italy) around 32,600 cal B.P. Proc. Natl. Acad. Sci. 112 (39), 12075–12080. https://doi.org/10.1073/pnas.1505213112.
Martínez-Sanz, M., Erboz, E., Fontes, C., López-Rubio, A., 2018. Valorization of Arundo donax for the production of high performance lignocellulosic films. Carbohydr. Polym. 199, 276–285. https://doi.org/10.1016/j.carbpol.2018.07.029.
Mason, S.L.R., Hather, J.G., Hillman, G.C., 1994. Preliminary investigation of the plant macro-remains from Dolní Věstonice II, and its implications for the role of plant foods in Palaeolithic and Mesolithic Europe. Antiquity 68 (258), 48–57. https://doi.org/10.1017/S0003598X00046184.
McPartland, J.M., Hegman, W., Long, T., 2019. Cannabis in Asia: its center of origin and early cultivation, based on a synthesis of subfossil pollen and archaeobotanical studies. Veg. Hist. Archaeobotany 28 (6), 691–702. https://doi.org/10.1007/s00334-019-00731-8.
Mercader, J., 2009. Mozambican grass seed consumption during the Middle Stone Age. Science 326 (5960), 1680–1683. https://doi.org/10.1126/science.1173966.
Mercader, J., Akeju, T., Brown, M., Bundala, M., Collins, M.J., Copeland, L., et al., 2018. Exaggerated expectations in ancient starch research and the need for new taphonomic and authenticity criteria. FACETS 3 (1), 777–798. https://doi.org/10.1139/facets-2017-0126.
Messner, T.C., 2011. Acorns and Bitter Roots: Starch Grain Research in the Prehistoric Eastern Woodlands. University of Alabama Press.
Monnier, G., Frahm, E., Luo, B., Missal, K., 2017. Developing FTIR microspectroscopy for analysis of plant residues on stone tools. J. Archaeol. Sci. 78, 158–178. https://doi.org/10.1016/j.jas.2016.12.004.
Morrison, W.R., 1988. Lipids in cereal starches: a review. J. Cereal. Sci. 8 (1), 1–15. https://doi.org/10.1016/S0733-5210(88)80044-4.
Moss, G.E., 1976. The microscopy of Starch. In: Radley, J.A. (Ed.), Examination and Analysis of Starch and Starch Products. Springer, Dordrecht. https://doi.org/10.1007/978-94-010-1332-1_1.
Motuzaite-Matuzeviciute, G., Telizhenko, S., Jones, M.K., 2012. Archaeobotanical investigation of two Scythian-Sarmatian period pits in eastern Ukraine: implications for floodplain cereal cultivation. J. Field Archaeol. 37 (1), 51–60. https://doi.org/10.1179/0093469011Z.0000000004.
Nagy-Bodor, E., Jarai-Komlodi, M., Medve, A., 2000. Late Glacial and Post-Glacial pollen records and inferred climatic changes from Lake Balaton and the great Hungarian Plain. In: Hart, M.B. (Ed.), Climates: past and Present, 181. Special publications, London, pp. 121–133. Geological Society.
Nakhutsrishvili, G., Batsatsashvili, K., Bussmann, R.W., Rahman, I.U., Hart, R.E., Haq, S. M., 2022. The subalpine and alpine vegetation of the Georgian Caucasus-a first ethnobotanical and phytosociological synopsis. Ethnobot. Res. Appl. 23, 1–60.
Napier, J.A., Haslam, R.P., Beaudoin, F., Cahoon, E.B., 2014. Understanding and manipulating plant lipid composition: Metabolic engineering leads the way. Curr. Opin. Plant Biol. 19, 68–75. https://doi.org/10.1016/j.pbi.2014.04.001.
Olatoyan, J.O., Neumann, F.H., Orijemie, E.A., Sievers, C., Evans, M., Hattingh, T., Schoeman, M.H., 2023. Modern pollen- and phytolith-vegetation relationships at a wetland in northeastern South Africa. South Afr. J. Bot. 161. https://doi.org/10.1016/j.sajb.2023.08.025.
Ordoñez-Araque, R., Ramos-Guerrero, L., Vargas-Jentzsch, P., Romero-Bastidas, M., Rodríguez-Herrera, N., Vallejo-Holguín, R., Fuentes-Gualotuña, C., Ruales, J., 2024. Fatty acids and starch identification within minute archaeological fragments: qualitative investigation for assessing feasibility. Foods 13 (7), 1090. https://doi.org/10.3390/foods13071090.
Palchowdhury, S., Mukherjee, K., Maroncelli, M., 2022. Rapid water dynamics structures the OH-stretching spectra of solitary water in ionic liquids and dipolar solvents. J. Chem. Phys. 157 (8), 084502. https://doi.org/10.1063/5.0107348.
Pastor, K., Ilić, M., Vujić, D., Jovanović, D., Ačanski, M., 2020. Characterization of fatty acids in cereals and oilseeds from the Republic of Serbia by gas chromatography–mass spectrometry (GC/MS) with chemometrics. Anal. Lett. 53 (8), 1177–1189. https://doi.org/10.1080/00032719.2019.1700270.
Paterson, A.H., Kong, W., Johnston, R.M., Nabukalu, P., Wu, G., Poehlman, W.L., Goff, V. H., Isaacs, K., Lee, T.H., Guo, H., Zhang, D., 2020. The evolution of an invasive plant, Sorghum halepense L.('Johnsongrass'). Front. Genet. 11, 317. https://doi.org/10.3389/fgene.2020.00317.
Pearsall, D.M., 2000. Paleoethnobotany: a Handbook of Procedures, third ed. Routledge.
Pearsall, D.M., 2008. Plant domestication and the shift to agriculture in the Andes. In: Silverman, H., Isbell, W.H. (Eds.), The Handbook of South American Archaeology. Springer New York, New York, NY, pp. 105–120. https://doi.org/10.1007/978-0-387-74907-5_7.
Piperno, D.R., 2006. Phytoliths: a Comprehensive Guide for Archaeologists and Paleoecologists. ISBN 0759103844.
Piperno, D., Weiss, E., Holst, I., Nadel, D., 2004. Processing of wild cereal grains in the upper Palaeolithic revealed by starch grain analysis. Nature 430, 670–673.
Piperno, D.R., Flannery, K.V., 2001. The earliest archaeological maize (Zea mays L.) from highland Mexico: new accelerator mass spectrometry dates and their implications. Proc. Natl. Acad. Sci. 98 (4), 2101–2103. https://doi.org/10.1073/pnas.98.4.2101.
Piperno, D.R., Holst, I., 1998. The presence of starch grains on prehistoric stone tools from the humid neotropics: indications of early tuber use and agriculture in Panama. J. Archaeol. Sci. 25 (8), 765–776. https://doi.org/10.1006/jasc.1997.0258.
Power, R.C., Rosen, A.M., Nadel, D., 2014. The economic and ritual utilization of plants at the Raqefet Cave Natufian site: the evidence from phytoliths. J. Anthropol. Archaeol. 33, 49–65. https://doi.org/10.1016/j.jaa.2013.11.002.
Pérez, S., Bertoft, E., 2010. The molecular structures of starch components and their contribution to the architecture of starch granules: a comprehensive review. Starch Staerke 62, 389–420. https://doi.org/10.1002/star.201000013.
Prosser, F., Bertolli, F., Festi, A., 2009. Flora Illustrata del Monte Baldo. Edizioni Osiride, Rovereto (TN). ISBN 10: 8874981236.
Pryor, A.J.E., Steele, M., Jones, M.K., Svoboda, J., Beresford-Jones, D.G., 2013. Plant foods in the Upper Palaeolithic at Dolní Věstonice? Parenchyma redux. Antiquity 87 (338), 971–984. https://doi.org/10.1017/S0003598X00049802.
R Core Team, 2021. R: a Language and Environment for Statistical Computing. R Foundation for Statistical Computing, Vienna, Austria. http://www.R-project.org.
Revedin, A., Aranguren, B., Becattini, R., Longo, L., Marconi, E., Lippi, M.M., et al., 2010. Thirty-thousand-year-old evidence of plant food processing. Proc. Natl. Acad. Sci. U. S. A. 107, 18815–18819. https://doi.org/10.1073/pnas.1006993107.
Richerson, P.J., Boyd, R., Bettinger, R.L., 2001. Was agriculture impossible during the Pleistocene but mandatory during the Holocene? A climate change Hypothesis. Am. Antiq. 66, 387–411.
Riehl, S., Karakaya, D., Zeidi, M., et al., 2024. Contextualizing wild cereal harvesting at Middle Palaeolithic Ghar-e Boof in the southern Zagros. Sci. Rep. 14, 18748. https://doi.org/10.1038/s41598-024-69056-5.
Rull, V., 2022. Origin, early expansion, domestication and anthropogenic diffusion of Cannabis, with emphasis on Europe and the Iberian Peninsula. Perspectives in Plant Ecology. Evolution and Systematics 55, 125670. https://doi.org/10.1016/j.ppees.2022.125670.
Scarponi, P., Izzo, F.C., Bravi, M., Cavinato, C., 2021. C. vulgaris growth batch tests using winery waste digestate as promising raw material for biodiesel and stearin production. Waste Management 136, 266–272. https://doi.org/10.1016/j.wasman.2021.10.014.
Schmid, K.M., Ohlrogge, J.B., 2008. Chapter 4 - lipid metabolism in plants. In: Vance, Dennis E., Vance, Jean E. (Eds.), Biochemistry of Lipids, Lipoproteins and

Membranes, fifth ed. Elsevier, pp. 97–130. https://doi.org/10.1016/B978-044453219-0.50006-4. ISBN 9780444532190.

Shetty, S., Govindaraju, I., Siona Rebello, A., Chatterjee, D., Rahman, MdH., Mazumder, N., 2024. Chapter 1 - physicochemical modification and characterization of starch used in the food industry: a review. In: Mazumder, Nirmal (Ed.), Advanced Biophysical Techniques for Polysaccharides Characterization. Academic Press, pp. 1–46. https://doi.org/10.1016/B978-0-443-14042-6.00001-4.

Shillito, L.M., 2018. Phytolith analysis. In: Varela, S.L.L. (Ed.), The Encyclopedia of Archaeological Sciences. John Wiley & Sons, pp. 1–3. https://doi.org/10.1002/9781119188230.saseas0456.

Shuman, J.L., Cortes, D.F., Armenta, J.M., Pokrzywa, R.M., Mendes, P., Shulaev, V., 2010. Plant metabolomics by GC-MS and differential analysis. In: Plant Reverse Genetics: Methods and Protocols. Humana Press, Totowa, NJ, pp. 229–246.

Sistiaga, A., Mallol, C., Galván, B., Summons, R.E., 2014. The Neanderthal meal: a new perspective using faecal biomarkers. PLoS One 9 (6), e101045.

Slovak, M., Kučera, J., Turis, P., Zozomova-Lihova, J., 2012. Multiple glacial refugia and postglacial colonization routes inferred for a woodland geophyte, Cyclamen purpurascens: patterns concordant with the Pleistocene history of broadleaved and coniferous tree species. Biol. J. Linn. Soc. 105 (4), 741–760. https://doi.org/10.1111/j.1095-8312.2011.01826.x.

Soffer, O., 2004. Recovering perishable technologies through use wear on tools: preliminary evidence for Upper Paleolithic weaving and net making. Curr. Anthropol. 45 (3), 407–413. https://doi.org/10.1086/420907.

Spengler, R.N., Willcox, G., 2013. Archaeobotanical results from Sarazm, Tajikistan, an early Bronze Age Settlement on the edge: agriculture and exchange. Environ. Archaeol. 18 (3), 211–221. https://doi.org/10.1179/1749631413Y.0000000008.

Stahlschmidt, M.C., Collin, T.C., Fernandes, D.M., Bar-Oz, G., Belfer-Cohen, A., Gao, Z., et al., 2019. Ancient Mammalian and plant DNA from late Quaternary stalagmite layers at Solkota Cave, Georgia. Sci. Rep. 9, 6628. https://doi.org/10.1038/s41598-019-43147-0.

Sukenik, N., Iluz, D., Amar, Z., Varvak, A., Shamir, O., Ben-Yosef, E., 2021. Early evidence of royal purple dyed textile from Timna Valley (Israel). PLoS One 16 (1), e0245897. https://doi.org/10.1371/journal.pone.0245897.

ter Schure, A.T., Bruch, A.A., Kandel, A.W., Gasparyan, B., Bussmann, R.W., Brysting, A. K., de Boer, H.J., Boessenkool, S., 2022. Sedimentary ancient DNA metabarcoding as a tool for assessing prehistoric plant use at the Upper Paleolithic cave site Aghitu-3, Armenia. J. Hum. Evol. 172, 103258. https://doi.org/10.1016/j.jhevol.2022.103258.

Torrence, R., 2006. Starch and archaeology. In: Torrence, Barton (Ed.), Ancient Starch Research. Routledge, p. 17. https://doi.org/10.4324/9781315434896.

Trněný, O., Brus, J., Hradilová, I., Rathore, A., Das, R.R., Kopecký, P., Coyne, C.J., Reeves, P., Richards, C., Smýkal, P., 2018. Molecular evidence for two domestication events in the pea crop. Genes 9 (11), 535. https://doi.org/10.3390/genes9110535.

Urban, B., Bigga, G., 2015. Environmental reconstruction and biostratigraphy of Upper middle Pleistocene lakeshore deposits at Schoningen. J. Hum. Evol. 89, 57e70.

Ursin, V.M., 2003. Modification of plant lipids for human health: development of functional land-based Omega-3 fatty acids. J. Nutr. 133 (12), 4271–4274. https://doi.org/10.1093/jn/133.12.4271.

van Geel, B., Aptroot, A., Baittinger, C., Birks, H.H., Bull, I.D., Cross, H.B., Evershed, R.P., Gravendeel, B., Kompanje, E.J., Kuperus, P., Mol, D., 2008. The ecological implications of a Yakutian mammoth's last meal. Quaternary Research 69 (3), 361–376. https://doi.org/10.1016/j.yqres.2008.02.004.

van Zeist, W., Bottema, S., 2009. A palynological study of the Acheulian site of Gesher Benot Ya'aqov, Israel. Vegetation History and Archaebotany 18, 105–121. https://doi.org/10.1007/s00334-008-0167-5.

Wadley, L., Backwell, L., d'Errico, F., Sievers, C., 2020. Cooked starchy rhizomes in Africa 170 thousand years ago. Science 367, 87–91. https://doi.org/10.1126/science.aaz5926.

Wang, Min, Yang, Qing, Yang, Wanshu, Lin, Shi, Zhang, Yu, Zhou, Zining, Zhang, Wuqi, Zheng, Hongbo, 2022. Surface phytolith and pollen assemblages of a low-latitude subtropical region in Southwest China and their implications for vegetation and climate. Front. Plant Sci. 13. https://doi.org/10.3389/fpls.2022.1007612.

Wang, S., Chao, C., Cai, J., Niu, B., Copeland, L., Wang, S., 2020. Starch–lipid and starch–lipid–protein complexes: a comprehensive review. Compr. Rev. Food Sci. Food Saf. 19 (3), 1056–1079. https://doi.org/10.1111/1541-4337.12550.

Weiss, E., Kislev, M.E., Simchoni, O., Nadel, D., Tschauner, H., 2008. Plant-food preparation area on an upper Paleolithic brush hut floor at Ohalo II, Israel. J. Archaeol. Sci. 35 (8), 2400–2414. https://doi.org/10.1016/j.jas.2008.03.012.

Whelton, H.L., Hammann, S., Cramp, L.J., Dunne, J., Roffet-Salque, M., Evershed, R.P., 2021. A call for caution in the analysis of lipids and other small biomolecules from archaeological contexts. J. Archaeol. Sci. 132, 105397. https://doi.org/10.1016/j.jas.2021.105397.

Willerslev, E., Davison, J., Moora, M., Zobel, M., Coissac, E., Edwards, M.E., et al., 2014. Fifty thousand years of Arctic vegetation and megafaunal diet. Nature 506 (7486), 47–51. https://doi.org/10.1038/nature12921.

Wollstonecroft, M.M., Ellis, P.R., Hillman, G.C., et al., 2008. Advances in plant food processing in the near Eastern Epipalaeolithic and implications for improved edibility and nutrient bioaccessibility: an experimental assessment of Bolboschoenus maritimus (L.) Palla (sea club-rush). Veg. Hist. Archaeobotany 17 (Suppl. 1), 19–27. https://doi.org/10.1007/s00334-008-0162-x.

Yang, X., Perry, L., 2013. Identification of ancient starch grains from the tribe Triticeae in the North China plain. J. Archaeol. Sci. 40 (8), 3170–3177. https://doi.org/10.1016/j.jas.2013.04.004.

Zanina, O.G., Tur, S.S., Svyatko, S.V., Soenov, V.I., Borodovskiy, A.P., 2021. Plant food in the diet of the early Iron Age pastoralists of Altai: evidence from dental calculus and a grinding stone. J. Archaeol. Sci.: Report 35, 102740. https://doi.org/10.1016/j.jasrep.2020.102740.

Zhang, Y., Zhu, Y., Chen, J., Xia, C., Deng, J., Li, H., Li, Y., Li, J., Liu, P., 2018. Identification of three species commonly known as "daqingye" by internal leaf anatomy and high-performance liquid chromatography analyses. Acta Soc. Bot. Pol. 87 (1). https://doi.org/10.5586/asbp.3575.